Master of Science Thesis in Electrical Engineering
Department of Electrical Engineering, Linköping University, 2021

Model-based fault diagnosis of an electrical low-voltage grid

Johan Lindström

LINKÖPING UNIVERSITY

Master of Science Thesis in Electrical Engineering

Model-based fault diagnosis of an electrical low-voltage grid

Johan Lindström

LiTH-ISY-EX--21/5451--SE

Supervisor: **Daniel Jung**
ISY, Linköping university

Examiner: **Christofer Sundström**
ISY, Linköping university

Division of Vehicular Systems
Department of Electrical Engineering
Linköping University
SE-581 83 Linköping, Sweden

Sammanfattning

En tillförlitlig tillgång av elektricitet är nödvändig för det moderna samhällets grundläggande funktioner. Det är nödvändigt att fel och avvikelser i lågspänningsnät lätt kan upptäckas och diagnostiseras. Ett fel i ett elnät kan vara en konsekvens av flera orsaker, bland annat inre skador, tekniska fel, felaktiga elmätare och elstöld.

Den här uppsatsen undersöker möjligheterna med modellbaserade ansatser för feldiagnostik och övervakning av lågspänningsnät. Data och egenskaper från ett riktigt lågspänningsnät används i detta arbete. Dessutom införs hypotetiska sensorer i modellekvationerna och simuleringar. För att avgränsa och göra resultaten mer lättförståeliga används tre olika kluster, uppbyggda av ett fåtal hushåll och mellanliggande kablar, från nätet. Metoderna som används inkluderar modellering av detta lågspänningsnät, strukturell analys av isolerbarhetsprestanda för fel, och simulering av felscenarion i MATLAB. Undersökningen av isolerbarhetsprestandan använder isolerbarhetsmatriser och Dulmage-Mendelsohn decompostion.

Resultaten från den strukturella analysen visar att det är svårt att designa residualer som bara är känsliga för vissa fel och dra slutsatser om var ett visst fel äger rum. Många gånger visar det sig att flera fel inte kan isoleras från varandra. Slutsaten är att redundansen måste ökas i ekvationerna med ännu fler sensorer. Genom att använda den simulerade modellen direkt för residualgenerering kan tydligare och mer bestämda resultat ses. Eftersom den tar hänsyn till kvantiteter är det lättare att analysera och se efter förändringar i nätet. Ett fåtal introducerade sensorer kan ofta visa var en ström genom en kabel måste ha ökats. Ett injicerat fel kommer mer eller mindre alltid påverka residualer i direkt närhet. Eftersom fel kan uppstå i både sensorer och kablar är det ofta svårt att precisera varför och var felet uppstår.

Abstract

Reliable access to power is essential for modern society's fundamental functions. It is necessary that faults and abnormalities in low-voltage grids can easily be detected and diagnosed. A fault in a grid can be a consequence of several causes, including internal damage, technical errors, malfunctioning electricity meters and electricity theft.

This thesis investigates the possibilities with model-based approaches for fault diagnosis and monitoring of low-voltage grids. Data and properties from a real low-voltage grid is utilised in this thesis. Furthermore, hypothetical sensors are introduced in the model equations and simulations. To delimit and make the results easier to understand, three different clusters, made up from a few households and intermediate cables, from the grid are analysed. The methods used includes modelling of the real low-voltage grid, structural analysis of the isolability performance of faults, and simulation of faulty scenarios in MATLAB. The investigation of the isolability performance uses isolability matrices and Dulmage-Mendelsohn decomposition.

The results from the structural analysis show that it is hard to design residuals that are only sensible to certain faults and draw conclusions on where a particular fault takes place. Many times, it shows that several faults cannot be isolable from each other. The redundancy has to be increased in the equations with even more sensors. By using the simulated model directly for residual generation, clearer and more determined results can be seen. Because it does take quantities into account, it is easier to analyse and look after changes in the grid. A few introduced sensors can often tell where a current through a cable must have been increased. An injected fault will more or less always affect residuals in direct proximity. However, because faults can occur in both sensors and cables, it is often hard to specify exactly why and where the fault takes place.

Acknowledgments

I want to thank my examiner Christofer Sundström for all the technical input, and discussions about the theory and methods of my work.

I also want to thank my supervisor Daniel Jung for the continuous feedback throughout the work, and for all the meetings we had during this time. The discussions we have had have always been interesting. I have learnt a lot and am grateful to have had the opportunity to do this work.

Linköping, December 2021
Johan Lindström

Contents

Notation

Electric quantities

Notation	Meaning
I	Current
S	Power
U	Voltage
Z	Impedance
R	Resistance
X	Reactance

Abbreviations

Abbreviation	Meaning
DMD	Dulmage-Mendelsohn decomposition
FDT	Fault diagnosis toolbox
FBSM	Forward backward sweep method

1 Introduction

This thesis has been carried out at the department of Electrical Engineering, ISY, at Linköpings universitet in the spring of 2021. It covers an investigation of the possibilities with model-based approaches for diagnosis of electrical low-voltage grids. This chapter will cover a description of what faults can occur in a low-voltage grid, and the reason for their occurrence. Then, an initial explanation of what fault diagnosis is, is introduced. After that, the purpose of this work and the method are presented. Limitations and related research are lastly presented.

1.1 Motivation and problem description

Reliable access to power is essential for modern society's fundamental functions. For example, data servers and telecommunication systems are both expected to function all hours of the day. Also, today's households require heating, continuous internet access, and charging of devices. Multiple areas need a secure supply of electricity. The usage of the electrical grids has also changed. Previously, power was produced in large and centralised power plants and then distributed to the consumer. Even though most of the power will still be produced in the same way, a near future will entail an increased amount of alternative energy sources, e.g., wind and solar. For example, during 2020, the number of solar power plants connected to the grid in Sweden increased by approximately 50 % [1]. Furthermore, more households will want to charge their electrical vehicles. In 2050, it is estimated that chargeable vehicles will account for at least 60 % of the total vehicle fleet in Sweden [2]. It is likely that low-voltage grids – the grid closest to the consumer – will be affected by an increasing degree of stress, which may cause faults in the grid. The causes can arise from several reasons, not just the changing use of electricity. A fault in a grid can be a consequence of several causes, e.g.: internal damage, technical errors, malfunctioning electricity

meters and electricity theft. The financial losses of the providers of electricity, as a result of non-technical financial losses, are vast. One report suggests that non-technical losses worldwide, where electricity theft and malfunctioning electricity meters are included, accounts for up to 96 billion dollars annually [3]. It is also approximated that 1 % of the current delivered are stolen [4]. Furthermore, smart grids based on digital technology, may be vulnerable to cyber-attacks [5]. The rapid change mentioned, and the problems arising from this change, justifies that it is necessary that faults and abnormalities in low-voltage grids can easily be detected and diagnosed.

1.1.1 Fault diagnosis

The delivery of electricity should be conducted in a predictable and reliable way. Malfunctioning electricity meters and electricity theft are two potential faults, and it is of interest to detect them. It is of importance for the provider that obtained sensor data of electrical consumption corresponds to the actual consumption. Moreover, to be able to predict the maintenance period and consequently reduce down-time, it is necessary that faults in low-voltage grids can easily be detected and diagnosed. In large systems – like a low-voltage grid – this is done with a fault diagnosis system. To achieve this, models over the grids also need to be reliable. If some kind of fault occurs in a system, the task of a fault diagnosis system is to notify that it happens, so-called fault detection, and where it happens, so-called fault isolation. The purpose of the fault diagnosis system is to ensure a reliable system with maximum run-time. Several fault detection methods exist, such as data-driven methods and model-based methods. Information about the shape of the grid, characteristics of the cables, properties of the transformer, hourly data of electrical power consumption for all households etc. are in this case available. Therefore, modelling of the grid is possible, and because of this, this thesis will focus on model-based approaches. In short, a model of a system is used to predict how a system works and behaves. The resulting estimated output of the model, or one part of the model, could thereafter be used together with a real measurement of the output from the real system. Subtracting the first result with the second result yields a residual. The idea is that if a residual deviates from zero, some kind of fault occurs [6]. Several residuals may be generated for the same system. By studying how the residuals behave, it is made possible that different faults in various parts of the system can be located. This is due to various faults affecting the residuals differently. It is difficult to manually construct diagnosis systems for large-scale models. To simplify the fault diagnosis when the system is large, structural methods are useful. Structural methods enable a systematic analysis of structural fault detection and isolation properties.

1.2 Purpose and method

The purpose and the main objective of this thesis is to investigate the possibilities with model-based approaches for fault diagnosis and monitoring of low-voltage

grids. The methods that will be used includes modelling of a low-voltage grid, analysis of the isolability performance of faults, and simulation of faulty scenarios. The fault diagnosis will be performed by representing the low-voltage grid structurally. The properties of the structural model will thereafter be analysed with structural methods [7]. The fault diagnosis will also be performed by simulating the grid. With the acquired results, it will be investigated whether it is possible to design a fault diagnosis system of the grid.

The thesis will utilise data of a real low-voltage grid in Sweden provided by Tekniska Verken. The acquired data and information of the grid includes exactly how a certain grid is built up, and what characteristics the different components have. E.g., length, area and impedances of the cables, properties of the transformer and connections between nodes. Furthermore, hourly data of electrical power consumption for all households are available. This includes data for every hour during an entire year. To highlight how the data during a smaller period of time can look like, consider Figure 1.2 where hourly consumption data for two arbitrary households during one week is shown. The structure of the used grid is shown in Figure 1.1. It is composed of 140 nodes, of which 82 of the nodes are households. Previous master theses have used the same grid; the modelling and simulation of the grid is therefore based on the same projects. This includes the equations describing the grid, and a solver developed to calculate different voltages, currents and power consumption in the grid. Electrical power consumption data from fault scenarios are not available and must therefore be simulated.

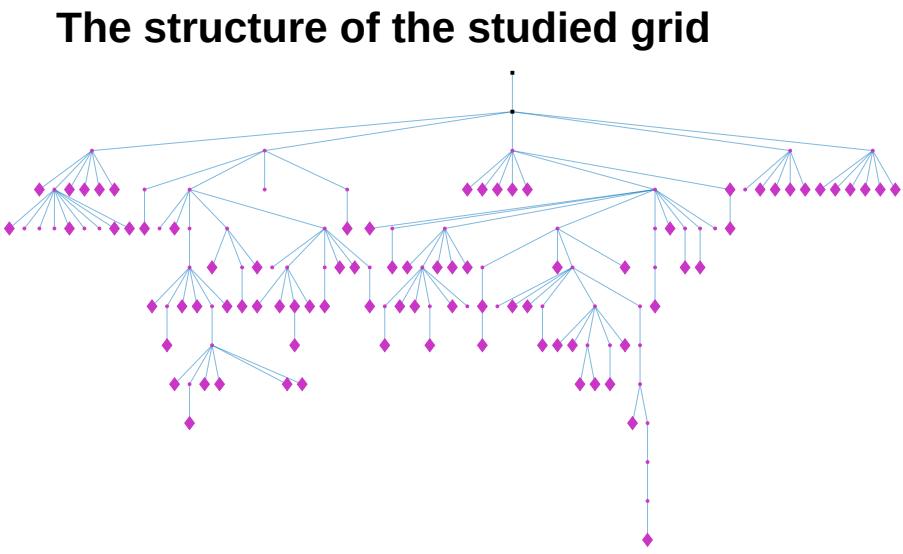

Figure 1.1: *The studied grid. The larger nodes are households.*

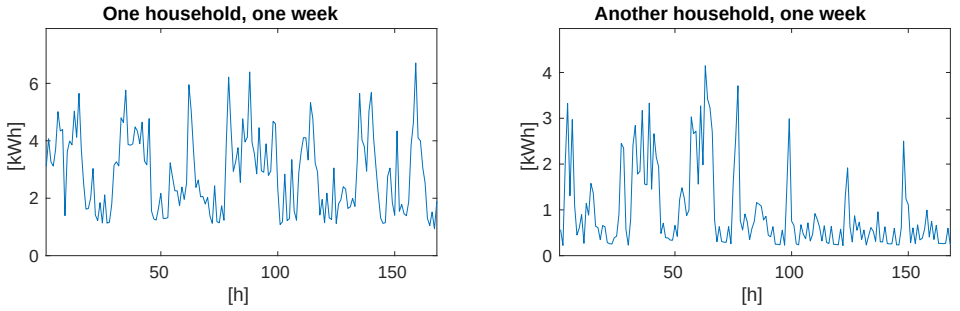

Figure 1.2: *Data for two arbitrary households during one week.*

1.2.1 Problem statements

The main objective of this thesis is to investigate the possibilities with model-based approaches for diagnosis and monitoring of low-voltage grids. The method will include structural analysis of fault detection and isolation using a model of a low-voltage grid. By using this model to generate residuals, an evaluation of the ability to detect and isolate faults will be conducted. The problem statements can be summarised as:

- What are the possibilities with model-based approaches for diagnosis of low-voltage grids?
- By using the model to generate residuals, an evaluation of the ability to detect and isolate faults will be conducted. This includes an analysis of fault detection and isolation using model of a low-voltage grid.

1.2.2 Limitations

The project will only cover a low-voltage grid. The transformer voltage is unknown, and is assumed constant. Furthermore, hourly data is in most cases available, but the result will only be presented in a selected hour. Due to the vastness of the grid, it is not possible to test and analyse all potential faults. Therefore, only some cases have been chosen for further investigation. Also, no real data exists from faulty cases. Consequently, this data will be simulated. Last, only one fault will be inserted in the simulation part. This fault will be a fixed increased power consumption, and will represent, for example, an electrical theft or a malfunctioning power meter.

1.3 Related research

The case study and grid simulation tools are based on results from previous master thesis projects. The first thesis [8] investigated how solar panels would affect the voltage variations in the grid. The second thesis [9] investigated how smart charging of batteries could support a grid. The third thesis [10] investigated if

the grid could be strengthened with batteries. This work differs in a way that its focus is fault detection. However, many aspects of the work, including the structure of the grid and the method to compute voltages and currents in the grid, will be used in this thesis.

Several studies of fault detection on electrical distribution grids have been conducted. In a review of distribution grid fault location techniques [11], the authors examine three different techniques, including travelling-wave methods and knowledge-based methods. Travelling-wave methods make use of several monitors that measure the difference of arrival time of travelling waves generated by faults. Knowledge-based methods can be summarised as methods where knowledge about the grid is utilised, e.g., the use of neural networks. The most prominent technique is however the impedance-based method, which in turn includes a few variations.

For example, the review mentions a report [12] where the authors describe an impedance-based method fault location algorithm. Several cases are discussed, but in short, the report suggests that by measuring voltages and currents over the fault, an assumed fault-loop impedance can be calculated. Thereafter, the impedance is calculated along the cable. Comparing the two estimated impedance will, with help of algorithms depending on fault type, give an estimation of the location of the fault. Furthermore, the authors have conducted a set of tests and can conclude that the fault location algorithm is effective.

One report [13] discusses the so-called fault metering. This term includes electricity theft and defected meters. A screening algorithm is being investigated. In short, energy usage, voltages and currents are measured several times each day. A rule-based model is thereafter used. It can be described as if- and then-expressions. Inside these expressions, a set of rules is stated. For example, voltage unbalance is a measured voltage subtracted by a reference voltage, then divided by the reference voltage. If the voltage unbalance is over a certain threshold, a certain number of times a day, it should alarm. An algorithm called Particle swarm optimisation is used, and it seeks to find the best parameters for the rule-based model. Tests are conducted and the authors can showcase satisfactory results in the fault metering.

Unlike the reports mentioned, this thesis will take a different route. This thesis will not in theory calculate an estimated distance to the fault, but use computed voltages to design residuals. Consequently, the thesis will look into if a given fault can impact residuals in direct proximity, and if some conclusions can be drawn from that analysis. To achieve this, the Fault Diagnosis Toolbox [14] will be used for modelling and analysis, something the related research have not used. Moreover, the residuals will not use some kind of impedance-based method, but instead utilise residual based fault diagnosis.

1.4 Thesis outline

The outline of this thesis is as follows:

- Chapter 2 provides theory behind the fundamental concepts of fault diag-

nosis. Moreover, in-depth concepts of structural analysis that will be used in the method are presented. Last, it is explained how the low-voltage grid will be modelled and adapted for fault diagnosis.

- Chapter 3 describes how the low-voltage grid was implemented in the used toolbox, and how it was simulated.
- Chapter 4 presents which parts of the low-voltage grid that was simulated, and thereafter the results from the tests conducted.
- Chapter 5 provides discussion of the findings in the result.
- Chapter 6 consists of the conclusion and potential future work.

2

Theory

This chapter seeks to explain the underlying theory of the methods that will be used in this thesis. First, theory about fault detection, and thereafter generation of residuals and their area of use for fault isolation, are introduced. Thereafter, the concepts of structural methods for analysis of large-scale non-linear models are presented. Last, an explanation of the modelling of the low-voltage grid is presented.

2.1 Fault diagnosis

The objective of this section is to describe fundamental concepts of model-based fault diagnosis. This includes modelling of faults, and how to detect and isolate faults using residual generators. Furthermore, the concepts of structural methods for analysis of large-scale non-linear models are presented.

2.1.1 Faults, detection and residual generators

Given a system, e.g., an electrical distribution grid. A fault can be described as when a property without allowance deviates from its nominal behaviour [6]. In the case of an electrical distribution grid, a fault that can be considered can, for example, be a larger current than expected. Consider Figure 2.1 where the value of an input into a system has a constant value of 1. The system is set to double the value of the input, i.e. the modelled expected value of the output is 2. However, some kind of fault occurs after 4 seconds. When measuring the output value with a sensor, it be noticed that the value of the output is 2 until 4 seconds, after that the value of the output is 3. The sensor measuring the output value notably differs from the predicted value, and the detection of a fault has been achieved.

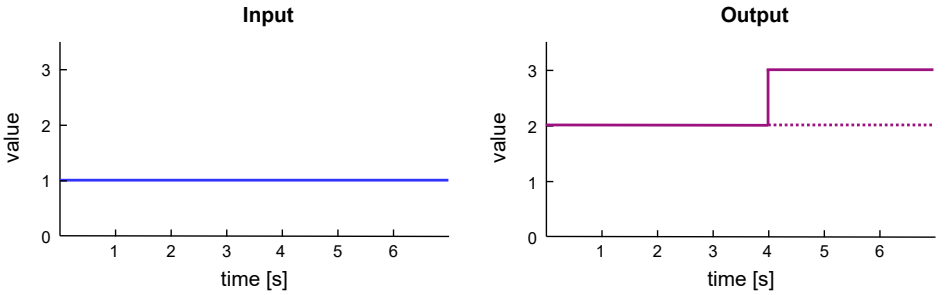

Figure 2.1: *Left: Value of the input into a system. The value of the input have a constant value of 1. Right: Value of the output from the same system, measured with a sensor. The value of the input is doubled until 4 seconds, thereafter tripled. The dotted line showcases the predicted behaviour of the output, i.e., a doubled input value.*

The usage of residuals is a convenient way to conduct model-based fault diagnosis. Initially, a model of a system is used to predict how a system works and behaves. The resulting estimated output of the model could thereafter be used together with a real measurement of the output from the real system [6]. The idea is that a comparison of the two values could result in valuable information about the location of a detected fault in the system. Residuals are generated by comparing a sensor output with a model prediction of the same signal. More exactly, the mathematically resulting residuals will in this thesis be described as follows:

$$r = y - \hat{y} \tag{2.1}$$

Where r is the residual, y is the measured sensor output and $\hat{y}$ is the estimated output from the model. To illustrate how a residual is generated from a true system and a model, consider the example shown in Figure 2.2. From an input, the measurement y from the system is subtracted by the estimated model output $\hat{y}$, and a residual is attained.

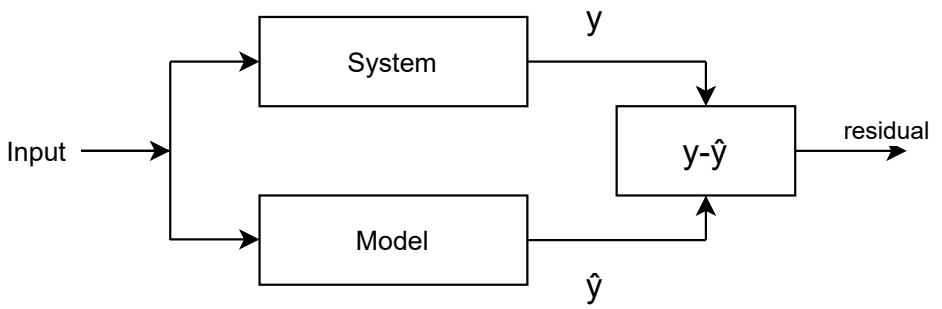

Figure 2.2: *Residual generation in an arbitrary time step.*

In terms of quantity, it is desirable to have a small difference between the output from the predicted model and the output from the true system – then the model is well constructed. The residual will be zero if the model is perfectly constructed. Since the model should be designed for a case without faults, a scenario with a fault in the true system would yield a residual that deviates from zero. To detect faults, alarms of potential faults can be set up with introduced thresholds:

$$|r| > J \tag{2.2}$$

Where r is the residual, and J is a threshold. An alarm is generated if the absolute value of the residual is larger than a given threshold.

2.1.2 Fault isolation

Fault isolation is defined as the localisation of different faults. By generating several residuals sensitive to different parts of the system, a study of which residuals that are affected can assist with the isolation of faults [6]. It is not always possible to isolate faults from each other, i.e., the generated residuals in a given system can be sensitive to more than one fault. To clarify what residuals can accomplish in terms of detection and isolation of faults, see Example 2.1.

Example 2.1

Consider the following model with an input signal, output signal and two sensors:

$$x_1 = 100 * u \tag{2.3a}$$
$$y_1 = x_1 \tag{2.3b}$$
$$y_2 = x_1 \tag{2.3c}$$

In (2.3), assume that u is the input signal and x_1 is the output signal. The output signal x_1 is measured with two sensors: y_1 and y_2. It is of interest to detect faults in the model, for that reason faults are modelled to the input signal and the two sensors in the following way:

$$x_1 = 100 * u + f_u \tag{2.4a}$$
$$y_1 = x_1 + f_1 \tag{2.4b}$$
$$y_2 = x_1 + f_2 \tag{2.4c}$$

In (2.4), assume that f_u is a fault from the input, f_1 a fault in the first sensor, and f_2 a fault in the second sensor. To detect the three modelled faults, residuals r_n – explained in Section 2.1.1 – are constructed by utilising (2.4).

$$r_1 = y_1 - 100 * u = f_1 + f_u \tag{2.5a}$$
$$r_2 = y_2 - 100 * u = f_2 + f_u \tag{2.5b}$$

The first residual r_1 contains both f_1 and f_u. Consequently, a fault in the first sensor will affect the first residual. The same goes for a fault from the input, which also will affect the first residual. Consequently, with the first residual, it is possible to detect both faults f_1 and f_u. However, it is not possible to isolate faults f_1 and f_u from each other with the first residual r_1. More exactly, the case of r_1 deviating from zero can be a consequence of f_1 and/or f_u, but is not possible to conclude exactly which one of the faults that affects the residual. Since the second residual r_2 contains both f_2 and f_u, the case of r_2 deviating from zero can be a consequence of f_2 and/or f_u, but it is not possible to conclude exactly which one of the faults that affects the residual. However, residual r_2 does not contain f_1; it is now possible to isolate f_1 from f_2.

2.1.3 Isolability matrix

As demonstrated in Example 2.1, a residual in a system may sometimes be sensitive to more than one fault. This results in it is not always possible to separate detected faults; one detected fault can be caused by another fault and vice versa. A comprehensible way to present which faults can be isolated from each other is by an isolability matrix [15]. An isolability matrix consists of rows with arbitrary fault modes, and columns with the same arbitrary fault modes. The intersection of a specific row and a specific column can be represented by a dot. A dot indicates what a fault can be caused by. The faults on the rows can be isolated to itself if there is only a dot to the same fault on the column. How well a specific fault can be isolated depends on how large the degree of redundancy is. For example, if the number of sensors – and residuals – in a system increases, it is often easier to isolate faults. To illustrate how an isolability matrix can be interpreted, consider an equation system where there are three detected faults, f_1, f_2 and f_3. The isolability matrix for this system is shown in Figure 2.3.

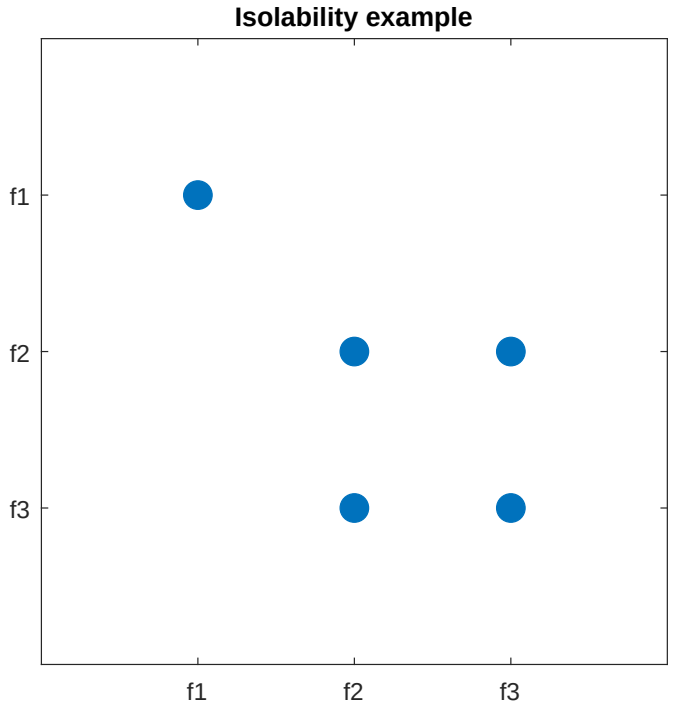

Figure 2.3: *Example of an isolability matrix where three fault variables, f_1, f_2 and f_3, are detected.*

In Figure 2.3, row f_1 only contains one dot – to column f_1; it can be isolated from both f_2 and f_3. However, row f_2 has dots on both column f_2 and column f_3; fault f_2 cannot be isolated from f_3. The same goes for row f_3, which has dots on both column f_2 and column f_3. How these faults can be isolated is clarified in the following table:

Table 2.1: *Isolability properties in Figure 2.3.*

Fault	Diagnosed to
f_1	f_1
f_2	f_2 and f_3
f_3	f_2 and f_3

An ideal case would be a diagonal isolability matrix. That would imply that all faults are isolable from each other.

2.1.4 Structural analysis

It is difficult to manually construct diagnosis systems for large-scale models. To simplify the fault diagnosis when the system is large, structural methods are use-

ful. The methods enable a systematic analysis of fault detection and isolation properties in an ideal case. In this thesis, the Fault diagnosis toolbox (FDT) [14] will be used for the structural analysis. The methods used are thoroughly described in [7]. The same equations as in (2.4) may be depicted structurally as in Figure 2.4.

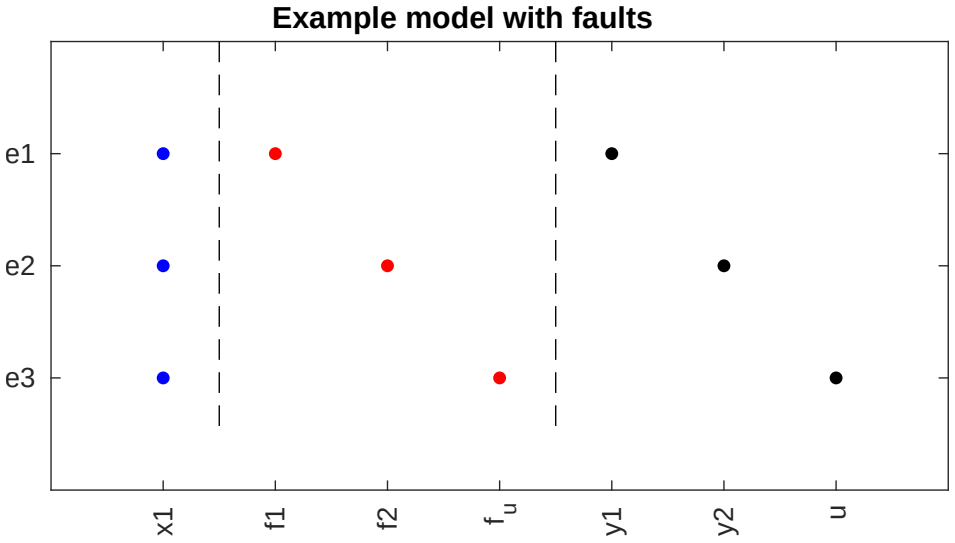

Figure 2.4: *The structure of* (2.4)*. Each row is one equation and each column is one variable. The columns on the left-hand side show the unknown variables, and the columns on the right-hand side show the known variables. The columns in the middle show the faults.*

The defined model structure as in Figure 2.4 contains unknown variables, known variables and faults. With structural methods, it can, for example, be studied if the model is redundant enough to detect certain faults.

2.1.5 Dulmage-Mendelsohn decomposition

The Dulmage-Mendelsohn decomposition [16] (DMD) is a way to reorder variables and equations in a given model. The composition does not add any additional variables or equations. The method and utilisation behind the DMD mentioned below is based on [7] and [17]. In short, given a model with equations M and unknown variables X, the form obtained after the decomposition can be seen in Figure 2.5.

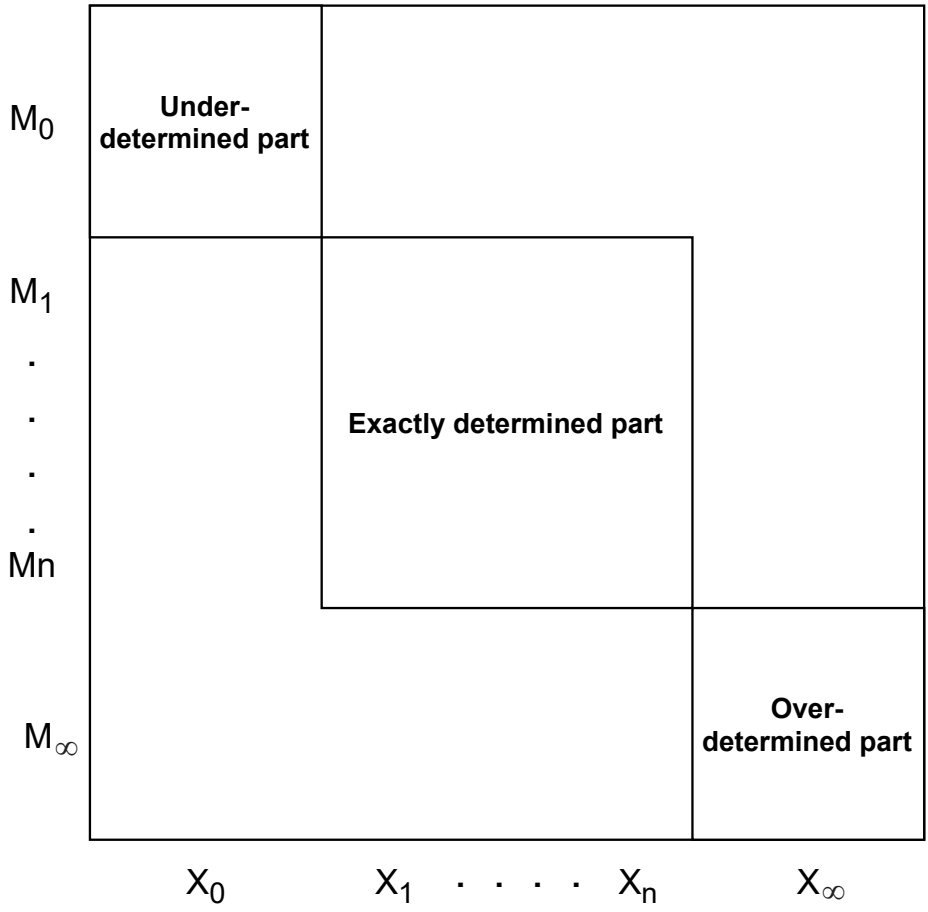

Figure 2.5: *Overview of a Dulmage-Mendelsohn decomposition (DMD). The y-axis shows the equations, and the x-axis shows the unknown variables. The decomposition is split into three blocks: an under-determined part, an exactly determined part and an over-determined part.*

As seen on the y-axis in Figure 2.5, the set of equations is split up into the parts $M_0, M_1, ..., M_n, M_\infty$, whereas the x-axis shows the different unknown variables split up into $X_0, X_1, ..., X_n, X_\infty$. Three fundamental parts of the DM are displayed:

- An **under-determined part** (M_0, X_0), meaning there are fewer equations than unknown variables.
- An **exactly determined part** $(M_1...M_n, X_1...X_n)$, meaning there are exactly same number of equations and unknown variables.
- An **over-determined part** (M_∞, X_∞), meaning there are more equations than unknown variables.

To draw conclusions about detection and isolation of faults, redundancy is needed. It is not possible to diagnose faults in the under- and exactly determined parts. Because the over-determined part has more equations than unknown variables, it has a redundancy of equations and is of special interest. The over-determined part of the DMD can furthermore be partitioned into blocks. To clarify how the over-determined part of the DMD and its corresponding isolability matrix interact, see Example 2.2.

Example 2.2

Consider a case with five unknown variables, seven known variables, five faults and seven equations. An example is presented in Figure 2.6.

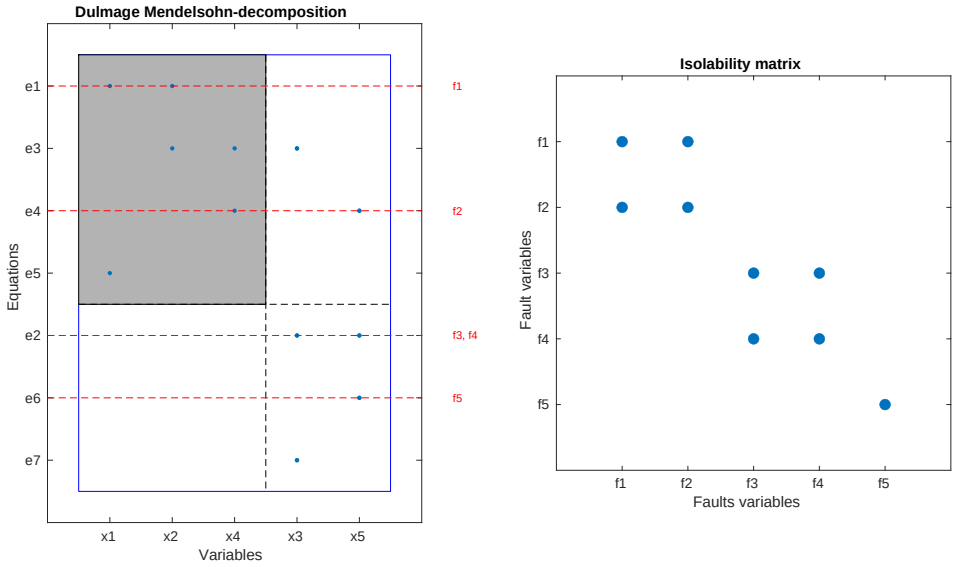

Figure 2.6: *Example case. Over-determined part of the DMD and its corresponding isolability matrix.*

In Figure 2.6, the over-determined part of the DMD has been partitioned into blocks. The blocks are $\{e1, e3, e4, e5\}$, $\{e2\}$, $\{e6\}$, and $\{e7\}$. It is worth noting that a block may just consist of one equation. If one equation is removed in the grey box, the redundancy is lost and all the equations in the box are removed from the over-determined part, i.e., all the equations in the block are needed. Consequently, if more than one fault appears in a grey box, they cannot be isolable, e.g., fault f_1 and f_2. This is also the case if a block only consists of one equation, e.g., fault f_3 and f_4 [14].

2.2 Modelling of low-voltage grid

To enable simulations and testing, modelling of the low-voltage grid will be performed in MATLAB. This is done by describing all the properties of the low-voltage grid by equations. To get a better understanding of how the grid will be presented, a small introductory example of the structure of a grid is illustrated in Figure 2.7.

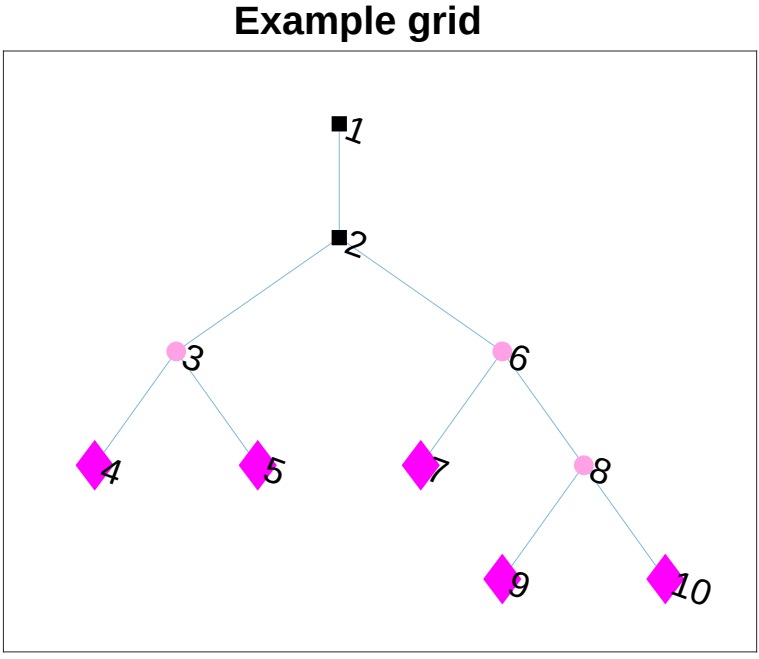

Figure 2.7: *Example of a grid. This is how the grid will be presented in the thesis. The first and the second node models a high-voltage side and a low-voltage side of a transformer, respectively. Nodes represented by a circle are regular nodes. Nodes represented by a diamond are load nodes.*

As seen in Figure 2.7, the grid will in this work be modelled by nodes and cables. The first node is a primary high-voltage side of a transformer, and the second node is the secondary low-voltage side of the same transformer. Nodes represented by circles will in this thesis be referred to as regular nodes, or just ***nodes***. The nodes do not contain households or electrical power consumption, and its sole purpose is to branch a cable. Nodes represented by a diamond will in this thesis be referred to as ***load nodes***, meaning they contain a household with a possible electrical consumption. To distinguish the nodes, they are given a unique number. If a certain node lies under, and is connected by a cable to, another node that is closer to the transformer, they will be referred to as a ***child*** and ***parent***. For example, in Figure 2.7, node 8 is a parent to load node 9 and load node 10. Load node 9 and load node 10 are children to node 8.

2.2.1 Modelling components

The modelling of low-voltage grids has been conducted in previous master theses [8] and [9]. This has been done as a balanced three-phase system. This work will use the same way of modelling the grid. The following equations describe the properties of the cables:

$$I_c = \frac{S}{\sqrt{3}U_h} \tag{2.6}$$

I_c is the current flowing through the cable, S is the power and U_h the voltage. Power loss in cables also need to be described:

$$S_{loss} = 3Z_c|I_c^2| \tag{2.7}$$

S_{loss} is the loss of power and Z_c the impedance in the cable. The impedance is a complex value :

$$Z_c = R + jX \tag{2.8}$$

R is the resistance and X is the reactance.
A voltage drop between two nodes is derived:

$$\Delta U = -\sqrt{3}I_c Z_c \tag{2.9}$$

The resulting voltage in a node will be described as:

$$U_{h,1} = U_{h,2} + \Delta U \tag{2.10}$$

$U_{h,1}$ is the voltage in a node, $U_{h,2}$ is the voltage in the preceding node.
Kirchoff's circuit law for currents is also used. Meaning the sum of all currents going into a node will be equal to the sum of all current going out.

$$\sum I_{in} = \sum I_{out} \tag{2.11}$$

2.2.2 Modelling faults and sensors

The grid presented in Section 2.2.1 is not modelled to enable structural analysis in FDT. For that reason, more equations are added to the already presented equations. First, equations for sensors measuring voltage and power are introduced. Some faults can also be found in the sensors, it is thereafter also necessary to introduce fault variables in the sensor equations. Equation (2.12) and equation (2.13) describe the introduced sensors and faults for voltage and power, respectively.

$$y_U = U + f_{y,U} \tag{2.12}$$

$$y_S = S + f_{y,S} \tag{2.13}$$

Where y_U and y_S are the sensors for voltage and power, respectively, and $f_{y,U}$ and $f_{y,S}$ are their accompanying sensor faults. Furthermore, it is also necessary to introduce fault variables in cables that will represent an unexpected increase of current flowing through the cable. This can, for example, be the theft of electricity. Equation (2.14) describes how this is done.

$$I_{c,out} = I_{c,in} + f_c \tag{2.14}$$

Where $I_{c,out}$ is the current flowing out from a node, and $I_{c,in}$ is the current flowing into the same node. f_c is the fault in the in-between cable describing the increased current.

2.2.3 Simulation of low-voltage grid

Data for power consumption in the low-voltage grid is available. To, e.g., produce voltage data in households, it needs to be simulated. To simulate the low-voltage grid, a method called Forward Backward Sweep Method is used (FBSM). The method is described in [18] and was implemented in a previous thesis [8]. The FBSM-solver is an iterative solver that uses the cable impedances Z, power usage S_{load} in all load nodes and a transformer voltage U_{tf}, as input. The solver outputs the voltages U, currents I and power S in all nodes. In Figure 2.8, an overview of the inputs and outputs can be seen.

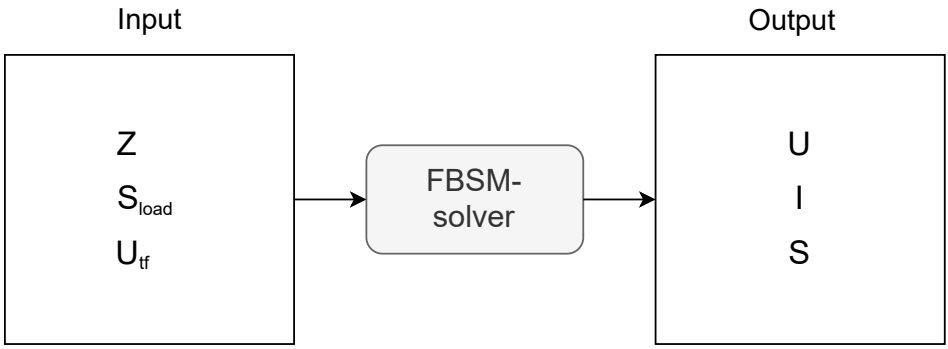

Figure 2.8: *An overview of which inputs the FBSM required, and which outputs it resulted in.*

3
Method

This chapter first describes how the model-based low-voltage grid structurally was implemented in the FDT. After that, it describes how it was simulated to in order to acquire more real-life scenarios.

3.1 Structural fault analysis

To structurally conduct fault analysis, the FDT described in [14] was utilised. The output used from the FDT was the DMD and the isolability matrix. In this analysis, fault variables and sensors as shown in Section 2.2.2 were introduced in every studied load node. This means that for every studied load node, sensors for voltage and power, and their corresponding faults were introduced. Furthermore, faults in all cables were also introduced.

3.1.1 Implementation of the grid into Fault Diagnosis Toolbox

When the FDT was used, it was first declared which unknown variables, known variables, faults, and parameters the grid was described by. These can be seen in Table 3.1

Table 3.1: *Variables used in the FDT.*

FDT variable	Meaning
x	Unknown variables
f	Faults
z	Known variables
parameters	Model parameters, for example cable impedances.

The grid consisted of a large quantity of nodes and cables, making it practically difficult and time-consuming to define every variable, property, and equation by hand. For this reason – based on information about how cables were connected, the properties of the cables, and the locality of the nodes – modelling of nodes and cables were done separately by a script. Thereafter, the modelled parts could be connected. This enabled the process of implementing the model of the grid in FDT to be done systematically. The resulting model was thereafter read into FDT. A flowchart of the process can be seen in Figure 3.1.

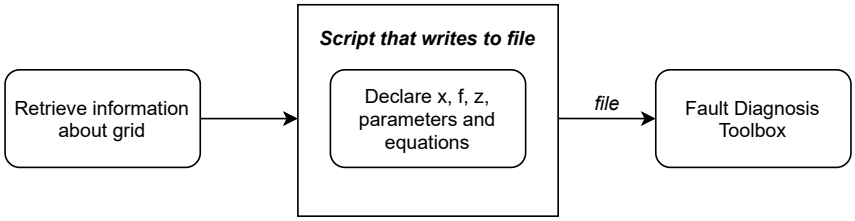

Figure 3.1: *Flowchart providing an overview of how the grid was implemented in FDT.*

An example of how a part of the file describing the variables, parameters and equations of a grid, looked like, can be seen in Figure 3.2. The code is abbreviated and only describes a small portion – two nodes – of the low-voltage grid. This is to give a sense of how the model is formulated.

```
% unknown variables
modelDef.x = {'Ic_3_4_in','Ic_3_4_out','Ic_2_3_out',...
              'S_3','S_4','deltaU_3_4','Uh_3','Uh_4'};
% faults
modelDef.f = {'f_3_4','f_Uh_3','f_Uh_4','f_S_3','f_S_4'};
% known variables (sensors)
modelDef.z = {'yS_3','yUh_3','yS_4','yUh_4'};
% grid parameters
modelDef.parameters = {'Z_ser_3_4','Y_shu_3_4'};

% model equations
modelDef.rels = {
S_3 == (sqrt(3)*Uh_3)*Ic_2_3_out, ...
S_4 == (sqrt(3)*Uh_4)*Ic_3_4_out, ...
Ic_3_4_out == Ic_3_4_in + f_3_4, ...
deltaU_3_4 == -sqrt(3)*(Ic_3_4_in*Z_ser_3_4), ...
Uh_4 == Uh_3 + deltaU_3_4, ...
yS_3 == S_3 + f_S_3, ...
yUh_3 == Uh_3 + f_Uh_3, ...
yS_4 == S_4 + f_S_4, ...
yUh_4 == Uh_4 + f_Uh_4, ...
};
```

Figure 3.2: *Example of how code used as input to FDT looked like. Variables and parameters are stated. The model equations describing the low-voltage grid are also defined.*

3.2 Simulation of the grid

The simulations made it possible to present the analysis in a way where the quantity of the residuals could be presented. As explained in Section 2.2.3, the FBSM-solver is an iterative solver that uses the cable impedances, power usage in all load nodes and a transformer voltage, as input. The FBSM-solver was run for all available time steps, but only some time steps were chosen to simplify the presentation of the results. A small concrete example of what the FBSM-solver calculates can be seen in Figure 3.3. The left part of the figure shows the initial information about the grid. Only power consumption data for load nodes is available. No data for voltage in load nodes, nor data for current running through cables, are available. The right part of the figure shows information about the grid after calculations with the FBSM-solver. Power consumption and voltage for load nodes, and currents, have been calculated.

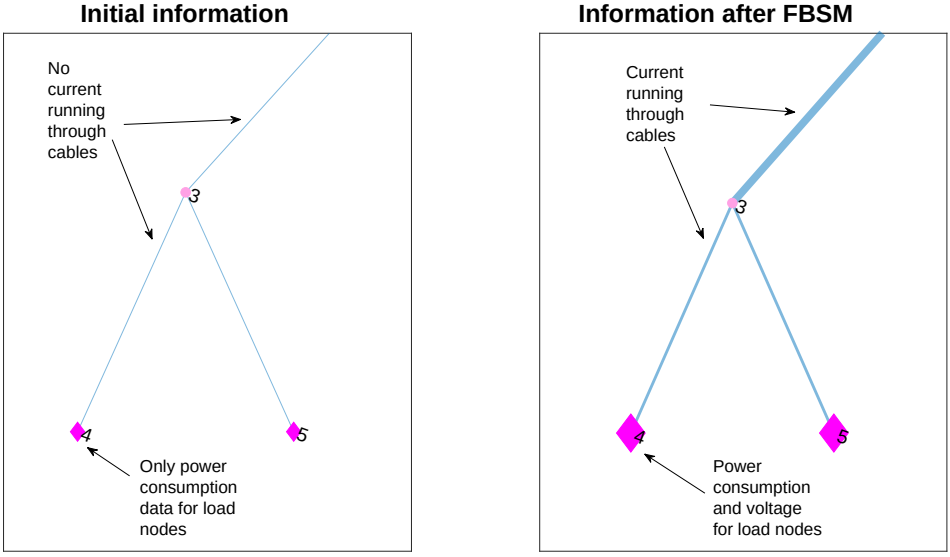

Figure 3.3: *A small example of what the FBSM-solver calculates. Left: Initial information about the grid. Only power consumption data for load nodes is available. Right: Information about the grid after calculations with the FBSM-solver. Power consumption and voltage for load nodes, and currents, have been calculated.*

3.2.1 Simulation of fault data

Since real sensor data with faulty cases are not available, a set of faulty scenarios are simulated. The attained original power consumption data was modified and utilised for this purpose. Furthermore, to simulate faulty cases where some kind of irregularity exists, the FBSM-solver presented in Section 3.2 was used. The original power consumption data was first taken. A selected load node was modified

by changing the power consumption. This could, for example, be increasing the power consumption in the household. This resulted in the original grid with a faulty load. After that, simulated sensor data in the grid from the faulty case need to be obtained. The FBSM-solver was run with the new grid – with a faulty load – as input. This resulted in simulated sensor data from a scenario with faulty load. The used approach can be seen in the flowchart in Figure 3.4.

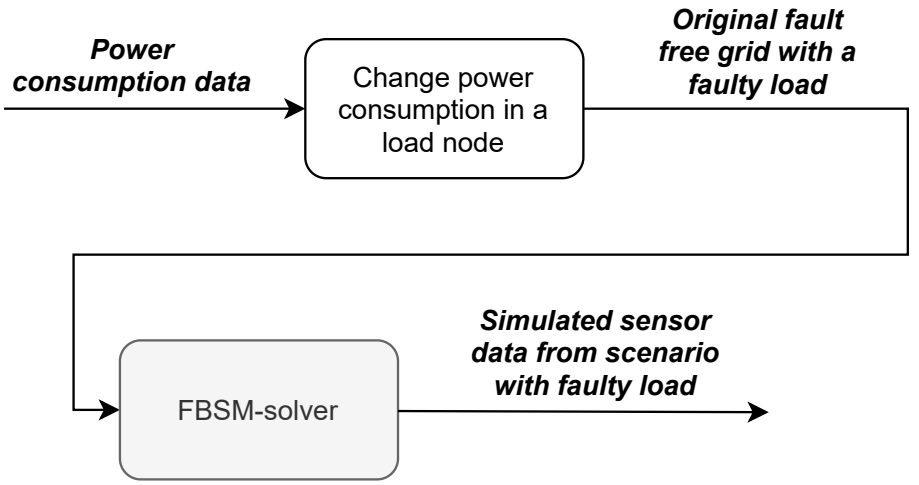

Figure 3.4: *Flowchart providing a workflow of how a simulated scenario with a faulty household consumption was created with the FBSM-solver.*

3.2.2 Residuals in the simulated environment

The voltage measurements from the simulated scenario with a faulty node are subtracted by the voltage measurements from the predicted model. In this way, residuals in arbitrary nodes were created.

$$r = y_U - \hat{y}_U \tag{3.1}$$

Where y_U are the voltage measurements from the simulated scenario with a faulty node, and $\hat{y}_U$ are the predicted voltage measurements. This method takes the entire model into account when predicting the voltage signals for the residuals. More exactly, no parts of the grid have been omitted when voltage signals have been calculated.

4

Result

In the following chapter, results are presented in two parts. The two parts will use one method each, and will later in the discussion be compared and discussed.

The first part consists of results from the **structural analysis** conducted in the FDT, i.e., the results in the first part are presented by DMD and isolability matrices. Sensors for voltage and power have been added. Also, the sensors' accompanying faults that represents, for example, malfunctioning electricity meters, have been added. Last, faults in cables that represent, for example, electricity theft have been added. The entire grid has been modelled, but only three clusters of nodes have been selected for further investigation. This is mainly because that a fault in the grid is assumed to have the greatest impact in the immediate vicinity. But also, because it was easier to present the results with a smaller cluster, rather than a vast grid.

The second part will also present the aforementioned three clusters, but in a **simulated environment** created by the FBSM-solver. The main difference between the first part and the second part is that different electrical quantities are showcased in the second part – unlike the first part where quantities were not taken into account. In the second part, for every cluster, four different scenarios have been chosen. Every scenario will show an increased power consumption in a different load node. The idea is to discuss which sensors are important for the isolation of faults.

4.1 Parts of the grid investigated

The analysis has been conducted on the entire grid. However, the vastness of the grid made it difficult to conduct tests, and to present the results, on the entire grid at the same time. For that reason, three different clusters with various appearances were chosen. This made it possible to methodically conduct tests

on just one cluster at a time and retain a good overlook of the result. The three clusters were used in both the structural analysis and the simulation tests. Table 4.1 shows which load nodes that belong to which cluster, and Figure 4.1 shows where the clusters are located in the studied grid. Furthermore, Figure 4.2, Figure 4.3 and Figure 4.4 show the appearances of cluster 1, cluster 2 and cluster 3, respectively. In the simulation part, each cluster was studied with four different scenarios. Each scenario meant that a different load node was modified with an increased power consumption.

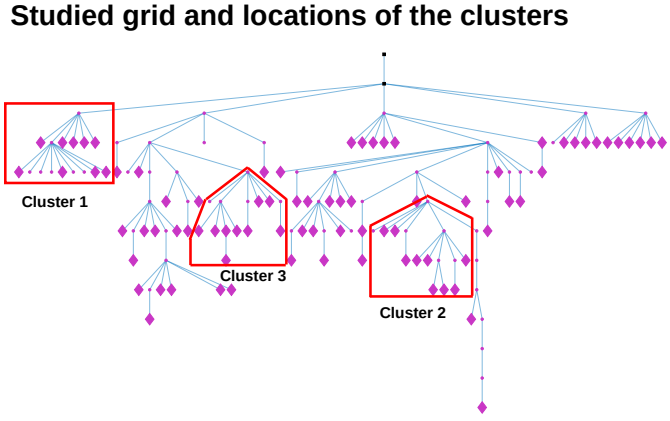

Figure 4.1: *Locations of the three clusters in the studied grid, highlighted in red.*

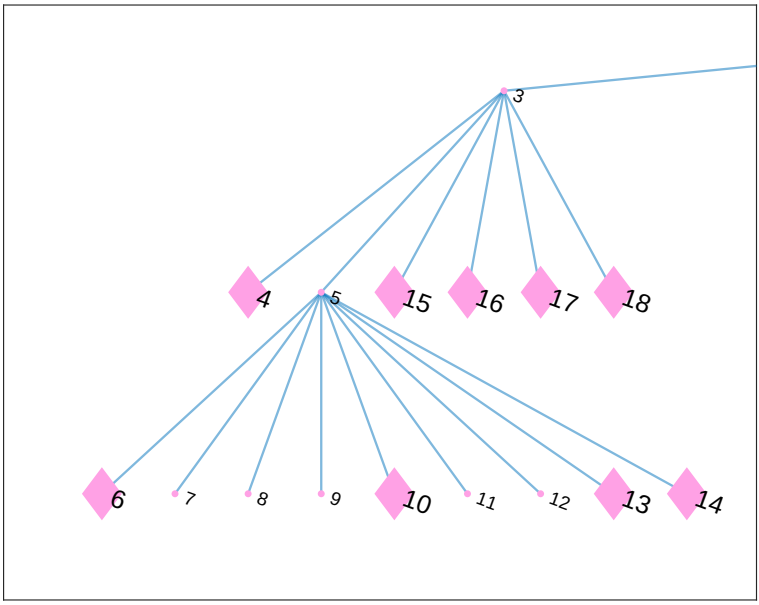

Figure 4.2: *The appearance of cluster 1. Load nodes are visualised with a diamond shape.*

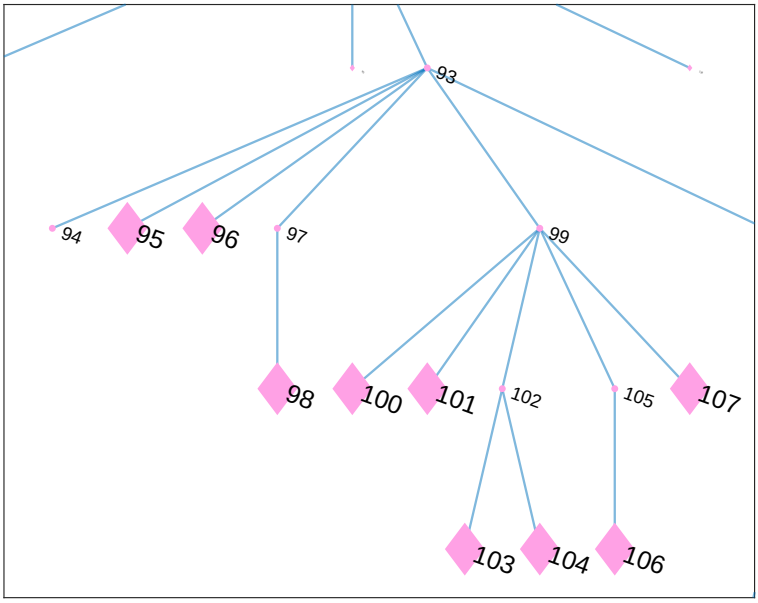

Figure 4.3: *The appearance of cluster 2. Load nodes are visualised with a diamond shape.*

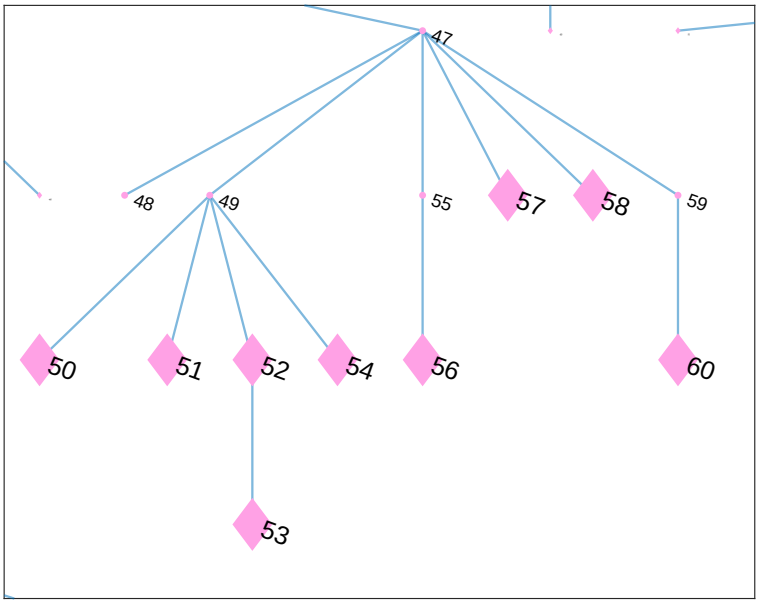

Figure 4.4: *The appearance of cluster 3. Load nodes are visualised with a diamond shape.*

Table 4.1: *Load nodes in the chosen clusters.*

Cluster	Load nodes
1	*4, 6, 10, 13, 14, 15, 16, 17, 18*
2	*95, 96, 98, 100, 101, 103, 104, 106, 107*
3	*50, 51, 52, 53, 54, 56, 57, 58, 60*

4.2 Structural analysis

This part presents the structural analysis produced in FDT. As a result of the vastness of the grid, there will be a large quantity of equations and variables. This makes the presentation of the results demanding. Consequently, all the DMD's will be zoomed into the over-determined part where sensors and faults have been injected, i.e., the cluster taken into consideration. Furthermore, the isolability matrix will be zoomed into the same part. As mentioned in Section 3.1, all the load nodes from the cluster taken into consideration, will be injected with two sensors and two faults. Also, the cables leading to or from the load nodes will be injected with one fault.

4.2.1 Cluster 1

The results from cluster 1 can be seen in Figure 4.5 and Figure 4.6. In both figures, a fault variable on the form $f_{U,m}$ represents an injected fault in the voltage sensor on node m, a fault variable on the form $f_{S,m}$ represents an injected fault in the power sensor on node m, and a fault variable on the form $f_{m,n}$ represents an injected fault in the cable between node m and node n.

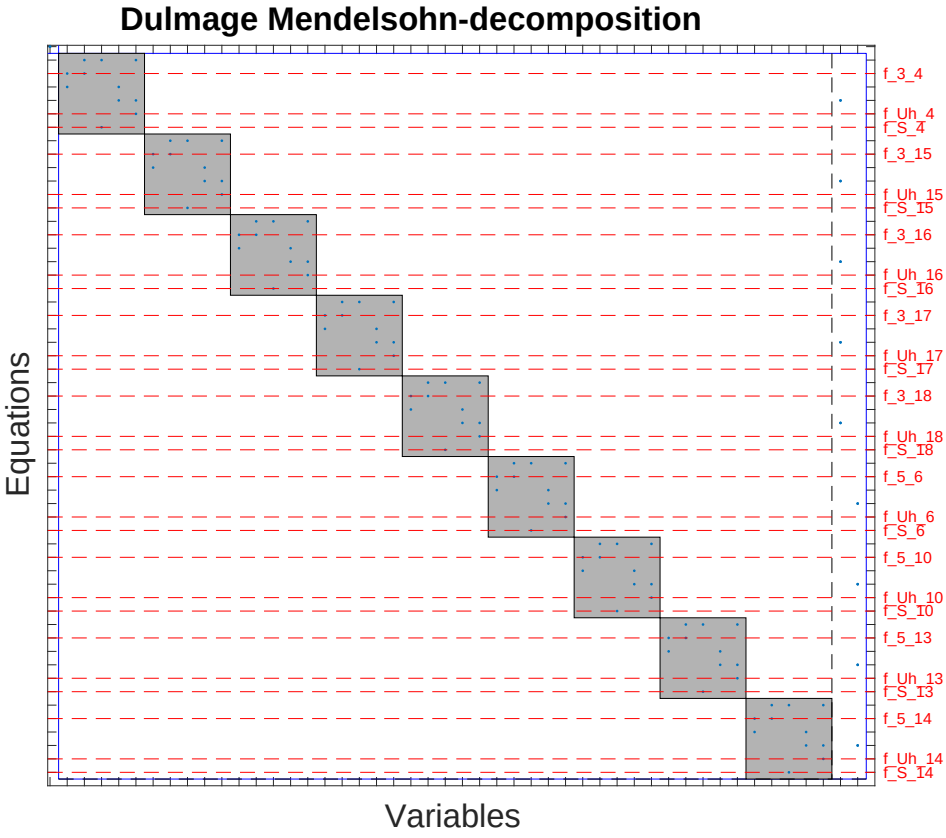

Figure 4.5: *Over-determined part of the DMD (cluster 1). Voltage sensors and power sensors on every load node in cluster. Faults in every sensor, and faults in every cable. Every row represents one equation the grid is modelled by. Every red line represents an injected fault, and the red lines are placed on the equation it is injected in. Every blue dot represents a variable of the grid.*

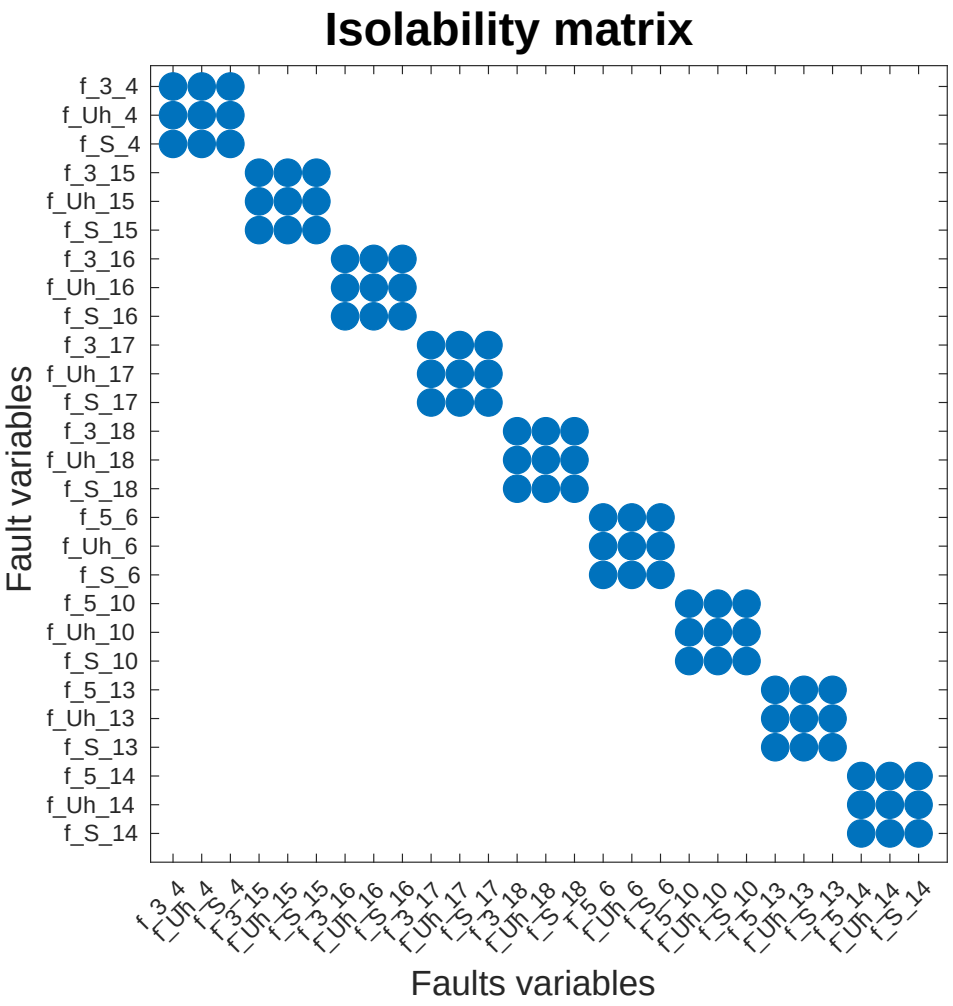

Figure 4.6: *The isolability matrix of cluster 1. Voltage sensors and power sensors on every load node in cluster. Faults in every sensor, and faults in every cable.*

As shown in Figure 4.5, the over-determined part of the DMD is split up into nine grey blocks – which are the same amount as load nodes. Three faults appear in every block: the fault in the voltage sensor, the fault in the power sensor, and the fault in the cable leading to that load node. A block always contains one more equation than unknown variables. All the equations are needed in a block to maintain the redundancy. At the same time, to isolate one fault from the other faults in the same block, the equations containing the other faults must be omitted – which results in lost redundancy. Consequently, faults in the same block cannot be isolated.

In the corresponding isolability matrix, Figure 4.6, the isolability properties

is shown more clearly. E.g., the fault in the cable leading from node 3 to load node 4, $f_{3,4}$, cannot be isolated from the sensor faults on load node 4, $f_{U,4}$ and $f_{S,4}$. The same behaviour can be seen for all load nodes throughout the cluster.

4.2.2 Cluster 2

The results from cluster 2 can be seen in Figure 4.7 and Figure 4.8. In both figures, a fault variable on the form $f_{U,m}$ represents an injected fault in the voltage sensor on node m, a fault variable on the form $f_{S,m}$ represents an injected fault in the power sensor on node m, and a fault variable on the form $f_{m,n}$ represents an injected fault in the cable between node m and node n.

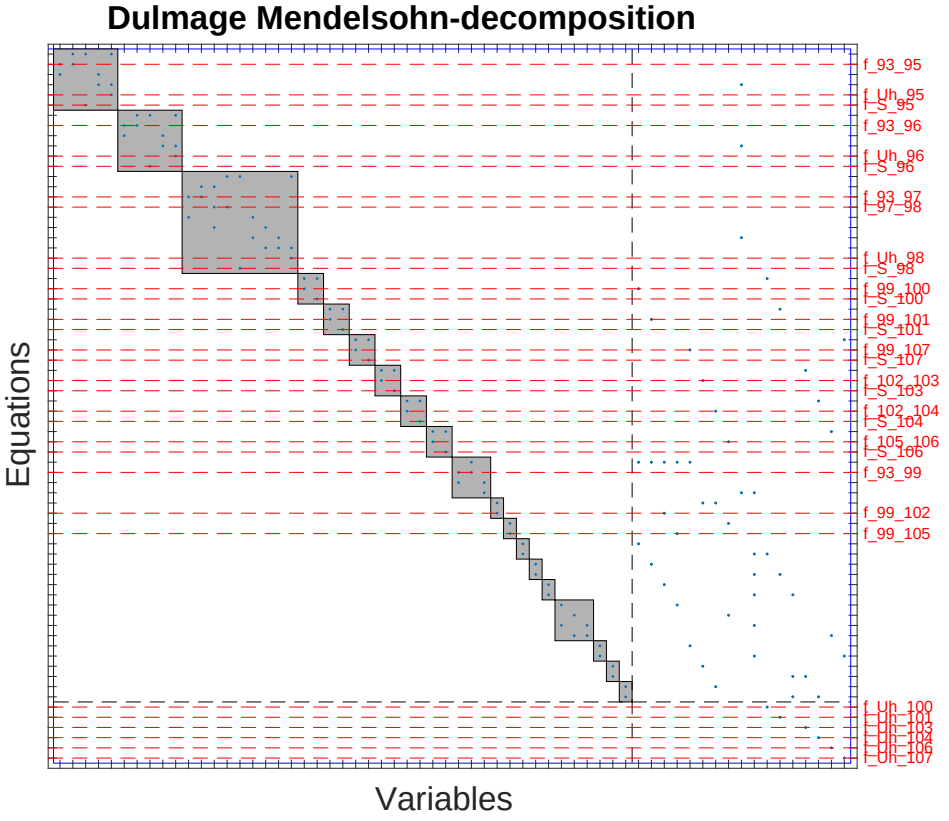

Figure 4.7: *Over-determined part of the DMD (cluster 2). Voltage sensors and power sensors on every load node in cluster. Faults in every sensor, and faults in every cable. Every row represents one equation the grid is modelled by. Every red line represents an injected fault, and the red lines are placed on the equation it is injected in. Every blue dot represents a variable of the grid.*

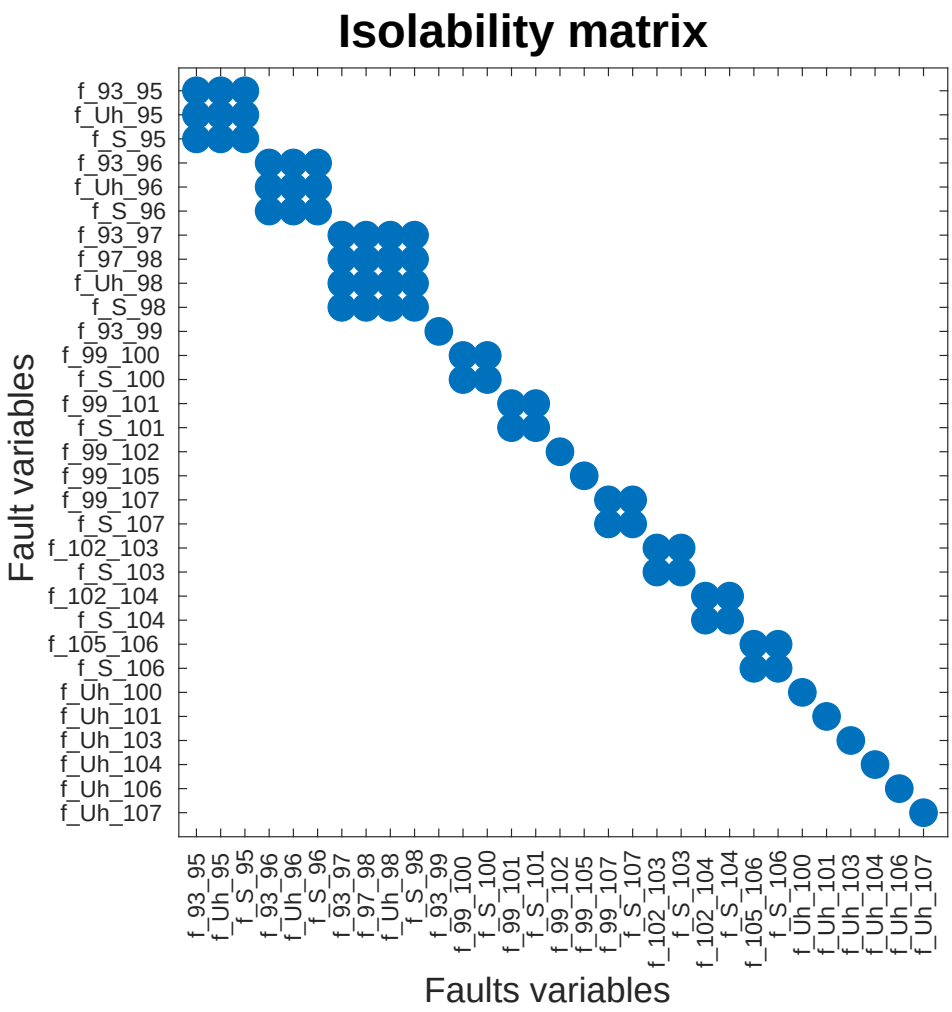

Figure 4.8: *The isolability matrix of cluster 2. Voltage sensors and power sensors on every load node in cluster. Faults in every sensor, and faults in every cable.*

As shown in Figure 4.7, the over-determined part of the DMD is split up into 25 different blocks. Some blocks are grey blocks containing several equations, and some blocks are single equation blocks (in the lower right corner). Worth noticing is that faults in cables between two nodes that are not load nodes are injected, namely, $f_{93,97}$, $f_{93,99}$, $f_{99,102}$ and $f_{99,105}$.

Examining the blocks, several constellations can be seen. Starting from the upper left corner, the first two blocks have three faults, a similar appearance as all the blocks in cluster 1. The third block is larger because it needs equations to describe an ”extra” cable, i.e., both the cable between node 93 and node 97, and the cable between node 97 and load node 98. Consequently, this block has one

more fault than the first two blocks. The following six blocks contain two faults each: one for the power sensor and one for the cable leading to that load node. The following three blocks contain one fault each. These faults are faults in cables between regular nodes. The last six blocks contain one fault each. These faults are all faults in voltage sensors. Seven blocks do not contain any fault. These blocks contain the equations with the variables describing the voltage drop ΔU – shown in (2.9) – from mainly node 99 to its child nodes. The main difference between cluster 1 and cluster 2 is that in cluster 2 – as shown in Figure 4.3 – node 99 is parent to three load nodes, but also parent two regular nodes, which in turn are parent to load nodes. Cluster 2 has three cables that separate the top node from the bottom load node, whereas cluster 1 – as shown in Figure 4.2 – has two cables. The different appearances between the clusters, where cluster 2 has a more complex connection of cables and nodes, make the structural results in cluster 2 differ from the results in cluster 1.

The corresponding isolability matrix, Figure 4.8, shows more clearly which faults that are isolable.

4.2.3 Cluster 3

The results from cluster 3 can be seen in Figure 4.9 and Figure 4.10. In both figures, a fault variable on the form $f_{U,m}$ represents an injected fault in the voltage sensor on node m, a fault variable on the form $f_{S,m}$ represents an injected fault in the power sensor on node m, and a fault variable on the form $f_{m,n}$ represents an injected fault in the cable between node m and node n.

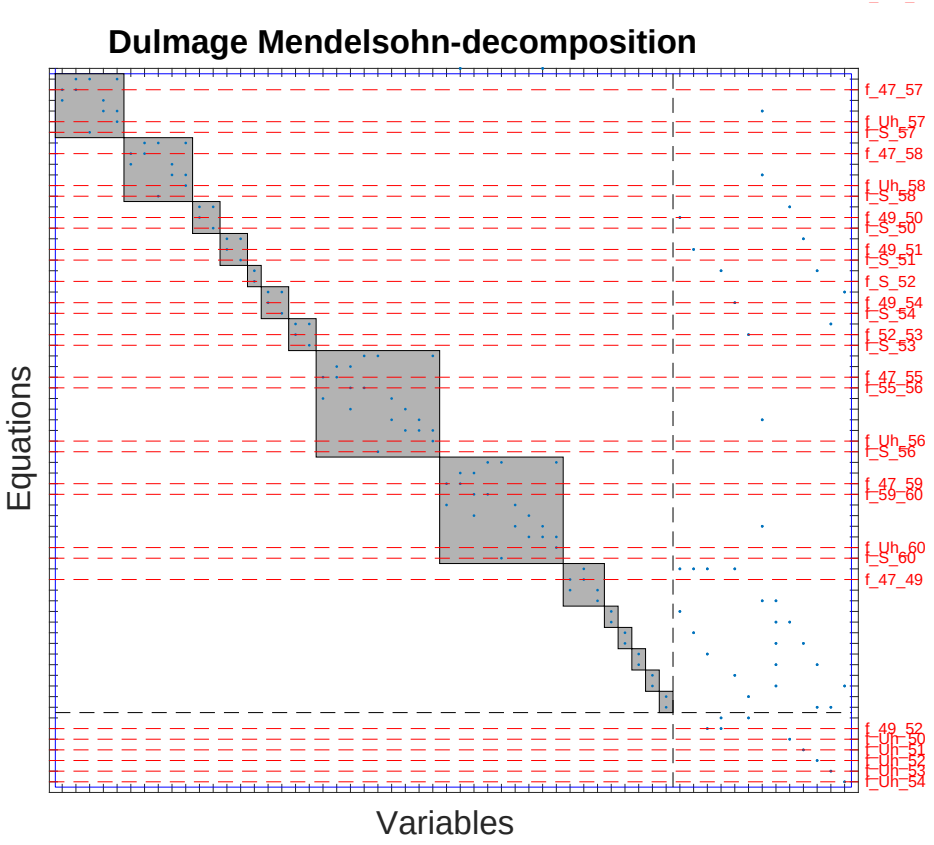

Figure 4.9: *Over-determined part of the DMD (cluster 3). Voltage sensors and power sensors on every load node in cluster. Faults in every sensor, and faults in every cable. Every row represents one equation the grid is modelled by. Every red line represents an injected fault, and the red lines are placed on the equation it is injected in. Every blue dot represents a variable of the grid.*

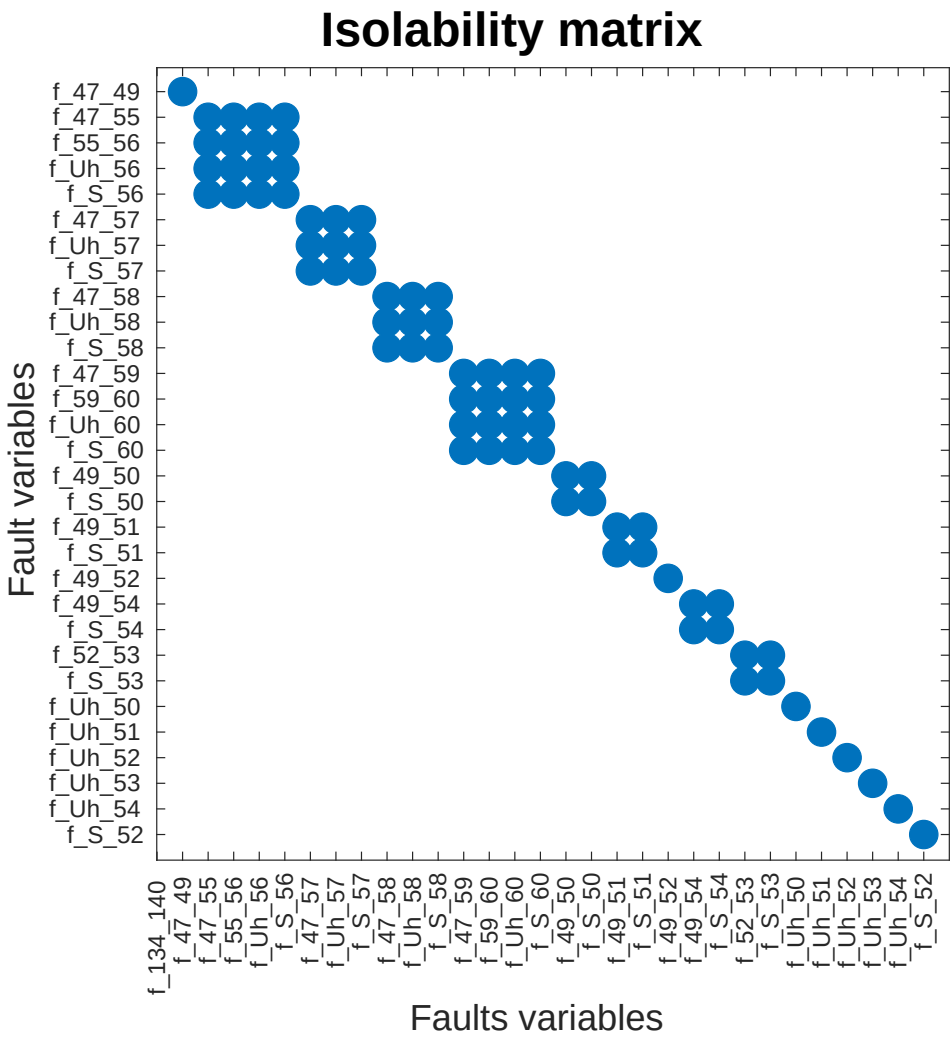

Figure 4.10: *The isolability matrix of cluster 3. Voltage sensors and power sensors on every load node in cluster. Faults in every sensor, and faults in every cable.*

As shown in Figure 4.9, the over-determined part of the DMD is split up into 21 different blocks. Just like cluster 2, some blocks are grey blocks containing several equations, and some blocks are single equation blocks (in the lower right corner). Again, worth noticing is that faults are injected in cables between two nodes that are not load nodes, namely, $f_{47,49}$, $f_{47,55}$ and $f_{47,59}$.

Examining the blocks, several constellations can be seen. Starting from the upper left corner, the first two blocks have three faults, a similar appearance as all the blocks in cluster 1. The following five blocks, with the exception from one block, have two faults. These blocks describe all the load nodes from 50 to

54. The exception with only one fault is load node 52. The following two blocks blocks are larger because they need equations to describe an ”extra” cable. These are the cables describing the region with node 47, node 55 and load node 56, and in the region with node 47, node 59 and load node 60. Consequently, these blocks have four faults. Common to these two blocks is that the structure is identical to the other large block shown in cluster 2. The appearances of the regions also points to this similarity. The following block contains only one fault, which is the fault in the cable from node 47 to node 49. The last six blocks contain one fault each. These faults are all faults in voltage sensors from load node 50 to load node 54, but also one fault in the cable from node 49 to node 52. Five blocks do not contain any fault. These blocks contain the equations with the variables describing the voltage drop ΔU – presented in (2.9) – from node 49 to its child nodes, and from load node 52 to load node 53.

Compared to cluster 2, this cluster shows many similarities: above all the uniquely isolable faults in the voltage sensors (in the bottom right corner of the results). Considering the appearances of the clusters, in Figure 4.3 and Figure 4.4, load node 100, load node 101, load node 103, load node 104, load node 106 and load node 107 in cluster 2, and load node 50, load node 51, load node 52, load node 53 and load node 54 in cluster 3, look similar.

The corresponding isolability matrix, Figure 4.10, shows more clearly which faults that are isolable.

4.3 Simulation results

For comparison, the same three clusters from the same grid presented in Section 4.1, were used in tests in a simulated environment. The main difference between the structural analysis part and the simulation part is that different electrical quantities are showcased in the simulation part – unlike the structural analysis part where quantities were not taken into account. The results in this part are based on the method presented in Section 3.2. In the faulty scenarios, it is simulated that one household in the cluster consumes significantly more power than expected. For every cluster, four different faulty scenarios where different load nodes consume significantly more power, are presented. In the presented results, all the nodes are numbered. If a node is studied with a sensor, it is highlighted with a diamond. The voltage differences calculated from the residual are showcased by a colour scale.

4.3.1 Cluster 1

A faulty scenario in cluster 1 means that the power consumption was increased by 1 kW on a load node. In Figure 4.11, the results from four different scenarios are presented. Load nodes are highlighted with diamonds.

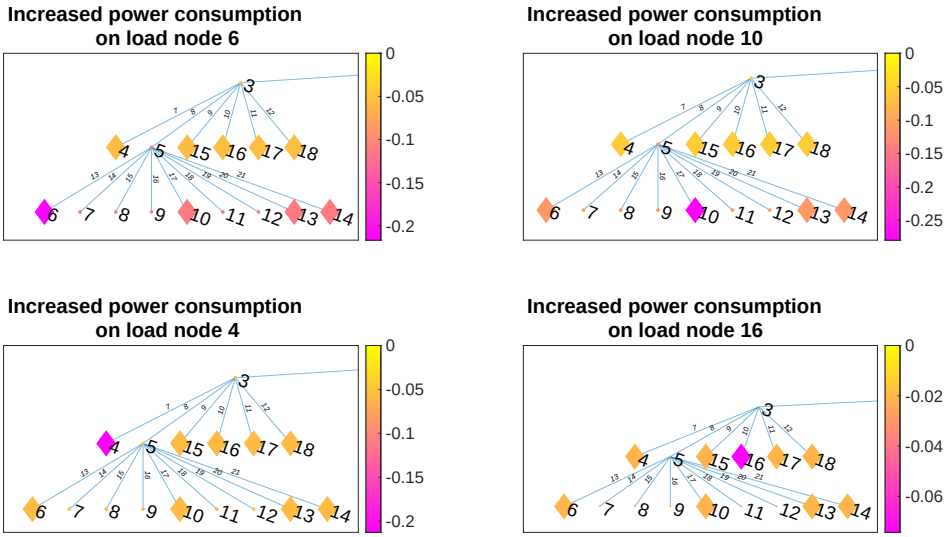

Figure 4.11: *Cluster 1, increased power consumption by 1 kW on selected load nodes. From upper left to lower right: scenario 1 (increased on load node 6), scenario 2 (increased on load node 10), scenario 3 (increased on load node 4) and scenario 4 (increased on load node 16).*

As shown in Figure 4.11, the scenario with an increased consumption on load node 6, showcases a voltage difference of approximately 0.2. The other load nodes originating from node 5 – load node 10, load node 13 and load node 14 – also showcase a substantial voltage difference, but lower than load node 6. The other load nodes – load node 4, load node 15, load node 16, load node 17 and load node 18 – showcase a small voltage difference. A nearly identical pattern can be seen in the scenario with an increased consumption on load node 10. The last two scenarios, with increased consumption on load node 4 and increased consumption on load node 16, showcase a voltage difference of approximately 0.2 and 0.06, respectively. All the other load nodes showcase a small voltage difference.

4.3.2 Cluster 2

A faulty scenario in cluster 2 means that the power consumption was increased by 1 kW on a load node. In Figure 4.12, the results from four different scenarios are presented. Load nodes are highlighted with diamonds.

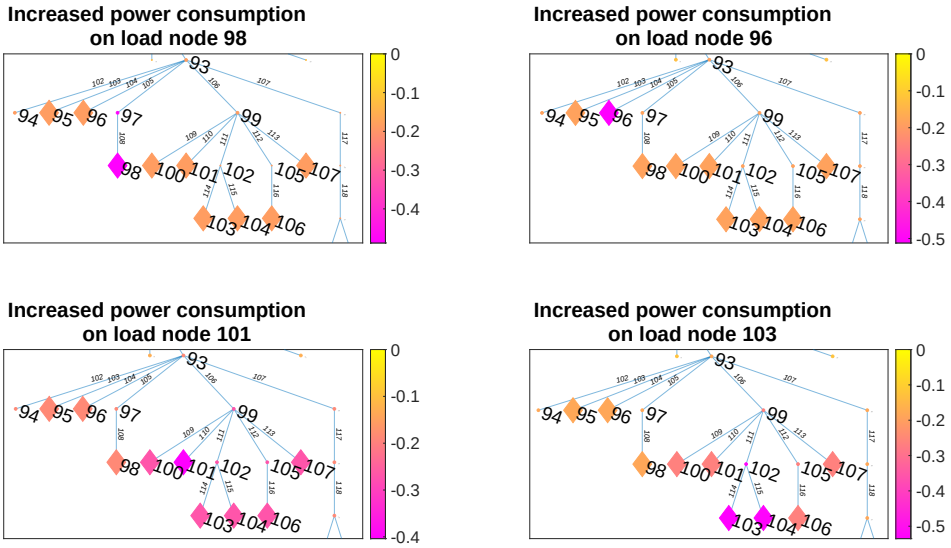

Figure 4.12: *Cluster 2, increased power consumption by 1 kW on selected load nodes. From upper left to lower right: scenario 1 (increased on load node 98), scenario 2 (increased on load node 96), scenario 3 (increased on load node 101) and scenario 4 (increased on load node 103).*

As shown in Figure 4.12, scenario 1 with increased consumption on load node 98 showcases a voltage difference of approximately 0.4. The other load nodes in the closest proximity – load node 95 and load node 96 – showcase a considerably smaller voltage difference, approximately 0.15. It is worth noticing that the faulty load node 98 is separated from them by three cables, and not two cables. The other load nodes with a much larger distance to the faulty load node – load node 100, load node 101, load node 103, load node 104, load node 106 and load node 107 – also showcase a considerable smaller voltage difference, also approximately 0.15. These are separated from the faulty load node 98 by at least four cables. The scenario with an increased consumption on load node 96 showcases a nearly identical pattern as the first scenario. The scenario with an increased consumption on load node 101 showcases a voltage difference of approximately 0.4. The load nodes in the closest proximity to load node 101 showcase a noticeable voltage difference of about 0.25, whereas the load nodes further away showcase a voltage difference of about 0.15. The fourth scenario with an increased consumption on load node 103 showcases a voltage difference of approximately 0.5. The same voltage difference can be is shown in the load node besides, load node 104. The other load nodes in the cluster showcase a smaller voltage difference: those in the closest proximity about 0.25 and those further away about 0.15.

4.3.3 Cluster 3

A faulty scenario in cluster 3 means that the power consumption was increased by 1 kW on a load node. In Figure 4.13, the results from four different scenarios are presented. Load nodes are highlighted with diamonds.

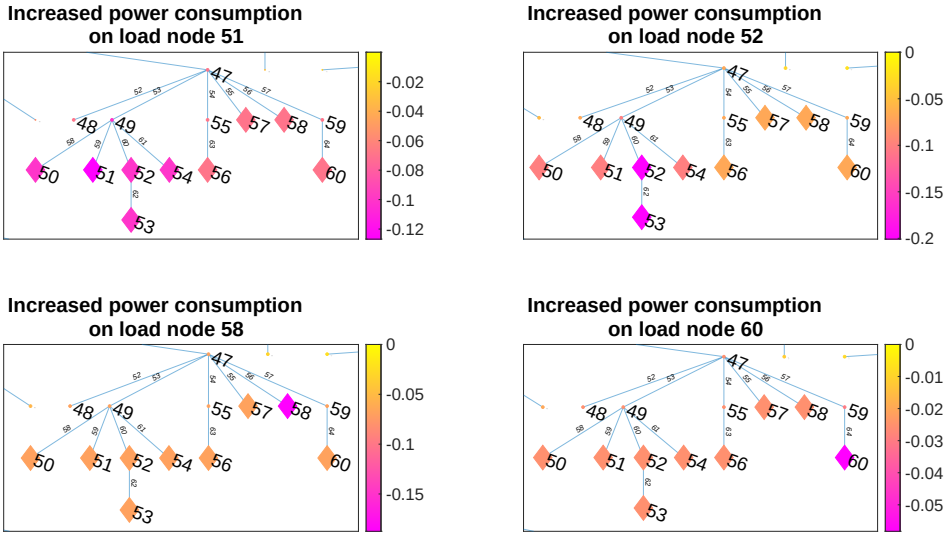

Figure 4.13: *Cluster 3, increased power consumption by 1 kW on selected load nodes. From upper left to lower right: scenario 1 (increased on load node 51), scenario 2 (increased on load node 52), scenario 3 (increased on load node 58) and scenario 4 (increased on load node 60).*

As shown in Figure 4.13, in scenario 1, load node 51 showcases a voltage difference of approximately 0.12. The other load nodes originating from load node 49 – load node 50, load node 52 and load node 54 – also showcase a voltage difference. However, the voltage difference in these load nodes are approximately in the same magnitude as on load node 51. The same voltage difference can also be seen on load node 53, which originates from the load node 52 and is separated from the faulty load node 51 by three cables. The rest of the load nodes in the cluster – load node 56, load node 57, load node 58 and load node 60 – showcase a smaller voltage difference of approximately 0.06. These are separated from the faulty load node of at least three cables. The second scenario where the power consumption has been increased in load node 52 showcases a voltage difference of about 0.2 in the faulty load node. Load node 53, which is directly connected to the faulty load node 52, also showcase a voltage difference of about 0.2. The rest of the load nodes originating from node 49 showcase a difference of about 0.1, whereas the rest of the load nodes further away showcase a voltage difference of under 0.1. The last two scenarios, with increased consumption on load node 58 and increased consumption on load node 60, showcase a voltage difference of approximately 0.2 and 0.06, respectively. All the other load nodes showcase a

substantial smaller voltage difference.

5
Discussion

This chapter consists of discussion regarding the results presented in Chapter 4. First, the results from Section 4.2 are discussed. Thereafter, results from Section 4.3 are discussed. Last, similarities and differences between the two parts are discussed. The purpose and problem statements stated in Section 1.2 and is the foundation for the discussion.

5.1 Results from the structural analysis

The results from the different clusters in the structural analysis in Section 4.2 differed regarding the isolability performance. The three clusters were chosen so that a wide range of different appearances and properties could be included.

Cluster 1

Cluster 1 in Section 4.2.1 consisted of nine load nodes. Cluster 1 originated from a parent node, with load nodes two levels down; the load node furthest from the parent node is separated by two cables. The fault in a cable leading to an arbitrary load node was never able to isolate from a fault in a voltage sensor or power sensor in the same load node. For example, neither the faults in the sensors on load node 14, $f_{S,14}$ and $f_{U,14}$, or the faults in the cable leading to load node 14, $f_{5,14}$, could be isolated from each other. The results showed that this was the case for all load nodes. To be able to exactly locate a fault in this cluster, the redundancy of equations needs to be larger in the affected area.

Cluster 2

Cluster 2 in Section 4.2.2 also consisted of nine load nodes. However, the structure of the cluster differed from cluster 1. Cluster 2 originated from a parent

node, with load nodes three different levels down; the load node furthest from the parent node is separated by three cables. The over-determined part of the DMD showed 25 different blocks. The first two blocks exhibited the same structure as all the blocks in cluster 1: three faults in every block. This is due to them describing load node 95 and load node 96, which are just one cable away from the parent node 93. It was not possible to isolate faults associated with node 93, node 97 and load node 98, and the DMD showed that four different faults appeared in the same block. This is due to node 97 not being a load node – it does not have any accompanying sensors. Furthermore, the existence of node 97 entails two cables with two accompanying cable faults. It is thus problematic when a **single** load node is separated from the highest node with intermediate nodes that are not load nodes. For example, if one new load node were to be introduced under node 97 and beside load node 98, its accompanying sensors would increase the redundancy. The rest of the blocks – containing the faults in the nodes in the interval 99 to 107, and faults in their accompanying cables – bring out diverse results. The faults in the voltage sensors from load nodes 100, 101, 103, 104, 106 and 107 are isolable. Furthermore, the faults in the cables between regular nodes are also uniquely isolable. It is not possible to isolate faults in a cable leading to a load node from the fault in the load node's power sensor. This is due to the power in, for example load node 100, being calculated by the current flowing into it. The fault in the cable has been injected into that equation: the equation of the current. The results clearly show that if the structure of the cluster includes, for example, more cables separating the load nodes from each other, the isolability properties change. This is mainly seen when the intermediate node is not a load node, and therefore does not have sensors.

Cluster 3

Cluster 3 in Section 4.2.3 also consisted of nine load nodes. Cluster 3 originated from a parent node, with load nodes three levels down. The over-determined part of the DMD showed 21 different blocks. The first two blocks exhibited the same structure as all the blocks in cluster 1: three faults in every block. This is due to them describing load node 57 and load node 58, which are just one cable away from the parent node 47. It was not possible to isolate faults associated with node 47, node 55 and load node 56. The same goes for node 47, node 59 and load node 60. Looking at how the cluster is built up, the appearances of load node 56 and load node 60 are identical. In both cases, the DMD showed that four different faults appeared in the same block. This is due to node 55 and node 59 not being load nodes – they do not have any accompanying sensors. Furthermore, the existence of node 55 and node 59 both entails two cables with two accompanying cable faults each. It is thus problematic when a **single** load node is separated from the highest node with intermediate nodes that are not load nodes. This case is identical to a case in cluster 2 previously discussed. The rest of the blocks showcase a diverse result. The faults in the voltage sensors from load nodes 50, 51, 52, 53 and 54 are isolable. With only one exception, it is not possible to isolate faults in a cable leading to a load node from the fault in the

load node's power sensor. This is the same result studied in cluster 2. Once again, this is due to the power in, for example load node 50, being calculated by the current flowing into it. The fault in the cable has been injected into that equation: the equation of the current. The only exception mentioned earlier is load node 52, where an interesting result can be seen. Load node 52 has load node 53 as a child. The two extra sensors load node 52 entail cause the redundancy to increase enough to make the fault on load node 52's power sensor isolable. Furthermore, the two extra sensors also cause the fault in the cable between node 49 and load node 52 to be isolable. Comparing this case to the case in cluster 2 – where a load node was separated from the top with an intermediate node, and not an intermediate load node – it is apparent that isolable performance is increased.

5.2 Results from the simulations

The results from the different simulations presented in Section 4.3 showed several occurrences worth mentioning. The faulty scenario in all tests were conducted by increasing the power consumption with 1 kW in a chosen load node.

Cluster 1

In cluster 1, the difference in voltage consumption in scenario 1, as seen in Figure 4.11, showed that the faulty load node 6 gave the largest indication. The voltage, described by (2.10), depends on the voltage drop, described by (2.9), which in turn depends on how much current, described by (2.6), flows into a node. A larger power consumption S will, according to (2.6), result in a larger current. This means that, in the case of a larger power consumption on load node 6, the current flowing from node 3 to node 5 must be increased. Consequently, the load nodes that also have node 5 as a parent node, will also be affected. Furthermore, the current flowing into node 3 must be higher. Load nodes 4, 15, 16, 17 and 18 will also be affected, but to a smaller degree. Thus, seeing a large voltage difference in, e.g., load node 6, but a small difference on load node 16, it is likely that the voltage drop occurs somewhere between node 3 and load node 6. Inversely, seeing a large voltage difference in, e.g., load node 16, but a small difference on load node 6 – as the fourth scenario shows – it can be assumed that the voltage drop occurs somewhere between node 3 and load node 16 – because a voltage drop before node 3 would yield a larger difference on load node 6. This realisation makes it easier to pinpoint approximately where the irregularity exists. Virtually the same can be said about scenario 2 and scenario 3.

Cluster 2

In cluster 2, the difference in voltage consumption in scenario 1, as seen in Figure 4.12, showed that the faulty load node 98 gave the largest voltage difference. By using the same conclusion about the voltage drop and current mentioned previously, the current flowing from node 93 to 97 needs to be increased. Node 97 also only have one child node: load node 98. Consequently, the difference on

load node 98 will stand out from the other nodes. The results show that this method works well when a faulty node is separated from other load nodes with more than one cable. If node 97, for example, had two more load nodes as children, it is likely to believe that these two also would display a larger voltage difference. This is due to the increased current flowing from node 93 to node 97. However, scenario 2 showed a similar result as scenario 1, even though load node 96 – which had the increased power consumption – was not separated from other load nodes with more than one cable. It is difficult to say why this happens, and it may be a coincidence. One reason may be the size of the initial power consumption, and the size of the increased power consumption. Looking at scenario 3, when the power consumption was increased on load node 101, the load nodes in the closest proximity showcase a substantial voltage difference. It can be assumed that the voltage drop occurs somewhere between node 93 and node 99. Comparing this to scenario 4, when the power consumption was increased on load node 103, load node 103 and load node 104 showcase the clearest voltage difference. Here, it can be assumed that the voltage drop occurs somewhere between node 99 and load node(s) 103/104. This reinforces the conclusion drawn earlier: this method works well when a faulty node is separated from other load nodes with more than one cable. However, because load node 103 and load node 104 are equally affected, it is not always possible to point out where the fault occurs.

Cluster 3

In cluster 3, the difference in voltage consumption in scenario 1, as seen in Figure 4.13, showed that the faulty load node 51 marginally indicated a larger difference than the other load nodes. Interestingly, e.g., load node 52 and load node 53 showed voltage differences that were hard to distinguish from the faulty load node 51. This may be a result of how the FBSM-solver calculated the voltages in this particular case. Again, the increased power consumption on load node 51 resulted in an increased current in the cable leading from node 47 to node 49. In this case, this gave a significant impact on node 49's children, even on load node 53 that is two levels down. Comparing this to the second scenario when the power consumption was increased on load node 52, it can be assumed that the fault occurs on either load node 52 or load node 53. Why it is easier to point out the fault in this case may be a result of load node 52 having a child. Furthermore, because the current was not increased to the same extent in the cable leading from node 47 to the rest of the nodes, it was easier to label which part of the cluster that did not have a faulty node. Looking at the third and fourth scenario, when the power consumption was increased in load node 58 and load node 60, a similar result can be seen: the affected load nodes showcase the largest voltage difference. However, the fourth case with load node 60 does not show this as clearly as load node 58. This may be a result of the initial power consumption in load node 60, i.e., it being large before the additional load.

5.3 Comparing the results from the two parts

By comparing the results from the structural analysis with the simulated results, consistent similarities and differences can be seen. For example, by looking at the structural analysis of cluster 1, it was theoretically possible to detect the three faults belonging to a load node: the fault in the voltage sensor, the fault in the power sensor, and the fault in the cable leading to that load node. However, they were not isolable from each other, meaning that it is not possible to know which kind of fault that affects. The simulation part of cluster 1, which measures the voltage difference, could detect that some change of voltage occurs. The difference in the simulation part is that is that a voltage difference sometimes can be seen in load nodes in proximity; the voltage difference is ”leaking” to nearby load nodes. The same pattern can be noticed by looking at the structural analysis of cluster 2, where it was theoretically possible to isolate the fault in the voltage sensor on load node 101. However, it was not possible to isolate the fault in the cable leading to load node 101 from the power sensor on load node 101. Looking at the simulated scenario with increased power on load node 101, the voltage difference was substantial on the load nodes nearby. Once again, the same pattern can be seen in cluster 3. By looking at the structural analysis of cluster 3, it was theoretically possible to isolate the fault in the voltage sensor on some nodes, e.g., load node 51. In the simulated part when the power consumption was increased on load node 51, all the load nodes nearby had a substantial voltage difference. It was impossible to locate where the consumption was increased. The results show that the structural analysis can provide good isolability properties. As a result of how the FBSM-solver works, the simulated part tends to show results where the difference leaks over to nearby nodes.

6

Conclusion and future work

This chapter consists of conclusions regarding the purpose and problem statements. Also, a section of potential future work and development is presented.

6.1 Conclusions

As stated in Section 1.1, the main objective of this thesis was to investigate the possibilities with model-based approaches for diagnosis and monitoring of low-voltage grids. The structural analysis and the generation of residuals would enable an evaluation of the ability to detect and isolate faults. A simulation of real-life faulty scenarios was also done, and thereafter compared with the results from structural analysis.

The information about cable parameters, properties of the transformer, connection between nodes and data from the power consumption in households, made it reasonable to use model-based approaches. The results from the structural analysis show that it is difficult to design residuals that are only sensible to certain faults. Theoretically, it could be seen that it was possible to detect and isolate faults down to the level where faults could be found in the grey blocks, or in a few cases isolate certain faults completely. The structural analysis works as intended, but it is limited by that it often shows that several faults cannot be isolable from each other. This is due to the equations modelling the grid being nested. To be able to uniquely isolate more faults, the redundancy has to be increased in the equations with even more sensors. From the structural analysis, it is difficult to design a diagnosis system. Mainly because it is challenging to draw conclusions on where a particular fault takes place.

By using the simulated model directly for residual generation, clearer and more determined results could be seen. Because it does take quantities into account, it is easier to analyse and look after changes in the grid. As mentioned in

the discussion, a few introduced sensors could often tell where a current through a cable must have been increased. An injected fault would more or less always affect residuals in direct proximity. This is due to how the FBSM-solver works. Furthermore, residuals and sensors far away from the fault showcased an insignificant change. However, because faults can occur in both sensors and cables, it is often difficult to specify exactly why and where the fault takes place. A diagnosis system of a low-voltage grid would, according to the results from the simulated residuals, probably be adequate in the case of excluding some parts of the grid. However, to exactly locate a fault, more work needs to be done. The results achieved show that there are possibilities with model-based diagnosis on a low-voltage grid. The results have also shown that the structural analysis and the simulated analysis bear similarities and differences. A future work could benefit from the similarities when residuals are created, i.e., a more methodical methodical and detailed review of the comparison could be done in a future work. This also includes a thorough examination of the various faults and other ways to generate residuals.

6.2 Future work

The subject and this project, can be developed further. Several potential ways to continue this work exists. Some suggestions are as follows:

- The simulation conducted in this work only took one kind of fault – the increased power consumption in one load node – into account. Numerous faulty scenarios exist, and one example of future work is looking into how several faults would affect the grid. For example, examine if two faults in proximity could be isolated.
- The impedance of the cables has a real part R and an imaginary part X. To imitate the behaviour of a broken cable, it could be of interest to investigate how the residual in a load node connected to cable is affected by the impedance. E.g., gradually increasing the resistance and reactance of the impedance, effectively increasing the voltage drop. This could be compared to cases where instead the current in a cable is gradually increased, resulting in that the voltage drop is increased.
- This work covers model-based methods. Other methods, for example, different algorithms, travelling-wave methods, or data-driven methods – where training data of fault cases may be collected and processed to achieve fault diagnosis, could be utilised. An investigation of whether one, or a combination of, the aforementioned methods, may be used to improve the fault diagnosis performance.

Bibliography

[1] Jeffrey Berard. 22 000 nya nätanslutna solcellsanläggningar. *Energimyndigheten*. URL https://www.energimyndigheten.se/nyhetsarkiv/2021/22-000-nya-natanslutna-solcellsanlaggningar-under-2020/.

[2] Energimyndigheten. Scenarier över sveriges energisystem 2020. URL https://energimyndigheten.a-w2m.se/Home.mvc?ResourceId=185971.

[3] LLC Northeast Group. Electricity theft and non-technical losses: Global markets, solutions, and vendors. URL http://www.northeast-group.com/reports/Brochure-Electricity%20Theft%20&%20Non-Technical%20Losses%20-%20Northeast%20Group.pdf.

[4] Thomas B Smith. Electricity theft: a comparative analysis. *Energy Policy*, 32(18):2067–2076, 2004. ISSN 0301-4215. doi: https://doi.org/10.1016/S0301-4215(03)00182-4. URL https://www.sciencedirect.com/science/article/pii/S0301421503001824.

[5] Tanzim Meraj, Shaela Sharmin, and Asif Mahmud. Studying the impacts of cyber-attack on smart grid. In *2015 2nd International Conference on Electrical Information and Communication Technologies (EICT)*, pages 461–466, 2015. doi: 10.1109/EICT.2015.7391997.

[6] Steven Ding. *Model-based Fault Diagnosis Techniques: Design Schemes, Algorithms, and Tools*. 01 2008. ISBN 978-3-540-76303-1. doi: 10.1007/978-3-540-76304-8.

[7] M. Krysander and E. Frisk. Sensor placement for fault diagnosis. *IEEE Transactions on Systems, Man, and Cybernetics - Part A: Systems and Humans*, 38(6):1398–1410, 2008. doi: 10.1109/TSMCA.2008.2003968.

[8] Johan Häggblom and Jonathan Jerner. Photovoltaic power production and energy storage systems in low-voltage power grids. Master's thesis, Linköpings universitet, 2019. URL http://urn.kb.se/resolve?urn=urn:nbn:se:liu:diva-156875. LiTH-ISY-EX–19/5194–SE.

[9] Mergim Dushku and Julius Kokko Ekholm. Charge into the future grid: Optimizing batteries to support the future low-voltage electrical grid. Master's thesis, Linköpings universitet, 2019. URL http://urn.kb.se/resolve?urn=urn:nbn:se:liu:diva-157358.

[10] Alexander Klasson and Philip Melin. Battery sizing and placement in the low voltage grid including photovoltaics. Master's thesis, Linköpings universitet, 2020. URL http://urn.kb.se/resolve?urn=urn:nbn:se:liu:diva-166795.

[11] Md Shafiullah and Mohammed Abido. A review on distribution grid fault location techniques. *Electric Power Components and Systems*, 45:1–18, 05 2017. doi: 10.1080/15325008.2017.1310772.

[12] M. M. Saha, F. Provoost, and E. Rosolowski. Fault location method for mv cable network. In *2001 Seventh International Conference on Developments in Power System Protection (IEE)*, pages 323–326, 2001. doi: 10.1049/cp:20010165.

[13] P. Fuangfung and P. Raphisak. Fault electricity metering detection using a rule-based model tuned by particle swarm optimization. In *2019 IEEE PES Asia-Pacific Power and Energy Engineering Conference (APPEEC)*, pages 1–5, 2019. doi: 10.1109/APPEEC45492.2019.8994450.

[14] Erik Frisk, Mattias Krysander, and Daniel Jung. A toolbox for analysis and design of model based diagnosis systems for large scale models. *IFAC-PapersOnLine*, 50(1):3287–3293, 2017. ISSN 2405-8963. doi: https://doi.org/10.1016/j.ifacol.2017.08.504. URL https://www.sciencedirect.com/science/article/pii/S2405896317308728. 20th IFAC World Congress.

[15] Dilek Düştegör, Erik Frisk, Vincent Cocquempot, Mattias Krysander, and Marcel Staroswiecki. Structural analysis of fault isolability in the damadics benchmark. *Control Engineering Practice*, 14(6):597–608, 2006. ISSN 0967-0661. doi: https://doi.org/10.1016/j.conengprac.2005.04.008. URL https://www.sciencedirect.com/science/article/pii/S0967066105001334. A Benchmark Study of Fault Diagnosis for an Industrial Actuator.

[16] A. L. Dulmage and N. S. Mendelsohn. Coverings of bipartite graphs. *Canadian Journal of Mathematics*, 10:517–534, 1958. doi: 10.4153/CJM-1958-052-0.

[17] Mattias Krysander, Jan Åslund, and Mattias Nyberg. An efficient algorithm for finding minimal overconstrained subsystems for model-based diagnosis. *IEEE Transactions on Systems, Man, and Cybernetics - Part A: Systems and Humans*, 38(1):197–206, 2008. doi: 10.1109/TSMCA.2007.909555.

[18] Xu Jingzhou and Chen Xiao. Forward/backward sweep method based on map structure for power flow calculation of distribution system. In *CICED 2010 Proceedings*, pages 1–4, 2010.